Biointerface Research in Applied Chemistry
Platinum Open Access Journal (ISSN: 2069-5837)

*Article*
**Volume 11, Issue 1, 2021, 7943 - 7972**
https://doi.org/10.33263/BRIAC111.79437972

# Anticancer Effect of Natural Product Sulforaphane by Targeting MAPK Signal through miRNA-1247-3p in Human Cervical Cancer Cells

**Meng Luo [1], Dian Fan [2], Yinan Xiao [2], Hao Zeng [2], Dingyue Zhang [2], Yunuo Zhao [2], Xuelei Ma [1,*]**

[1] Department of Biotherapy, State Key Laboratory of Biotherapy and Cancer Center, West China Hospital, Sichuan University, Chengdu, Sichuan 610041, P.R. China; luomeng_1017@163.com (L.M.);
[2] West China Medical School, West China Hospital, Sichuan University, Chengdu, Sichuan 610041, P.R. China; fan-dian@foxmail.com (F.D.); yinan_xiao@163.com (X.Y.N.); 13540285357@163.com (Z.H.); 2017141082017@stu.scu.edu.cn (Z.D.Y.); 2087247019@qq.com (Z.Y.N.);
* Correspondence: drmaxuelei@gmail.com;

Scopus Author ID 55523405000

**Received: 11.06.2020; Revised: 3.07.2020; Accepted: 5.07.2020; Published: 9.07.2020**

**Abstract:** The prognosis of cervical cancer remains poor. Sulforaphane, an active ingredient from cruciferous plants, has been identified as a potential anticancer agent in various cancers. However, there is little information about its effect on cervical cancer. Here, we conducted a present study to uncover the effect and the potential mechanisms of sulforaphane on cervical cancer. HeLa cells were treated with sulforaphane, and cell proliferation and apoptosis were assessed by Cell Counting Kit-8, Western blot, flow cytometry, and immunofluorescence. Then, next-generation sequencing (NGS) and bioinformatics tools were used to analyze mRNA-seq, miRNA-seq, and potential pathways. Finally, qRT-PCR, Cell Counting Kit-8, flow cytometry, small RNAs analysis, and Western blot were performed to evaluate the biological function of miR1247-3p and MAPK pathway in HeLa cell lines. Sulforaphane significantly suppressed the viability and induced apoptosis of HeLa cells. NGS and bioinformatics analysis showed sulforaphane exerted its anti-tumor activities through miR1247-3p and the MAPK signaling pathway. Further analysis suggested that sulforaphane could activate MAPK pathway via down-regulating the expression of miR-1247-3p. Sulforaphane inhibited proliferation and promoted apoptosis of HeLa cells via down-regulation of miR-1247-3p and activating the MAPK pathway. These findings provide preliminary experimental evidence for the treatment of cervical cancer with sulforaphane.

**Keywords:** Sulforaphane; Cervical cancer; Next-generation sequencing; Kyoto Encyclopedia of Genes and Genomes; MiR-1247-3p; MAPK pathway.

**List of Abbreviations**: CCK8 = cell counting kit 8, DMSO = dimethyl sulfoxide, GO = Gene Ontology, KEGG = Kyoto Encyclopedia of Genes and genomes, MAPK = mitogen-activated protein kinase, miRNA = microRNA, NGS = next-generation sequencing, qRT-PCR = quantitative real-time polymerase chain reaction, PI = propidium iodide



## 1. Introduction

Cervical cancer has become the fourth most common malignancy among women worldwide due to its high incidence and mortality rate[1] [2]. There are around 528,000 newly-diagnosed cervical cancer cases and 266,000 deaths every year, according to the latest global cancer statistics [3]. To date, effective treatments for patients with cervical cancer include surgery, chemotherapy, and radiotherapy[4]. Given many potential adverse side effects in these

traditional treatments, so it is worthwhile to search for a novel effective treatment for cervical cancer [5].

Sulforaphane, an herbal isothiocyanate typically abundant in cruciferous vegetables such as broccoli, cauliflower, and cabbage, has many biological effects such as anti-inflammation, anti-oxidation [6]. In particular, due to its anticarcinogenic role in pancreatic cancer, it has been noteworthy recently [7]. The antiproliferative and radiosensitizing properties for head and neck tumors also have been reported [8]. Although previous studies have identified the anti-tumor potential of sulforaphane in various kinds of cancers [9,10], the role of sulforaphane in cervical cancer has not been well recognized. MicroRNAs (miRNAs) are short, non-coding RNAs that play important roles in regulating many biological processes involving almost all aspects of cell physiology [11,12]. Typically, they regulate protein expression levels in physiological and pathophysiological processes by conjugating with complementary sequences of their target mRNAs[13,14]. As there are around 1000 miRNAs in the human genome, which modulate approximately one-third of the human genes[15], miRNAs are the most abundant regulators[16].

Accumulating evidence has shown that sulforaphane exerts its therapeutic effects through modulating the expression of cancer-related miRNAs on a variety of cancers, including colon cancer[17], lung cancer[18], gastric cancer[19], pancreatic cancer[20], skin cancer[21], acute myeloid leukemia[22], and nasopharyngeal cancer[23]. Besides, the previous study has demonstrated that miR-3156-3p, negatively associated with the incidence of HPV-positive cervical cancer, acted as a tumor-suppressive miRNA[24]. Furthermore, targeting MACC1, miR-338-3p could regulate the proliferation of cervical cancer cells via the MAPK pathway[25]. However, no elaborate research has found the association between miRNAs and sulforaphane in inhibiting cervical cancer until now. Therefore, given the anti-tumor capability of sulforaphane, we aimed at validating the anticancer activities and mechanisms of sulforaphane in cervical cancer, including downstream target miRNA and relevant signal pathway initiated by the miRNA.

In our study, we found that miR-1247-3p was highly related to both the apoptosis rate of cervical cancer cells cultured with sulforaphane and the activation of the MAPK pathway. Based on the high throughput sequencing and bioinformatics analysis, we ultimately disclosed the role of the miR-1247-3p-induced MAPK signal pathway in inhibition of cervical cancers treated with sulforaphane.

## 2. Materials and Methods

### *2.1. Materials.*

Sulforaphane was purchased from MedChem Express (#HY-13755, MCE, Monmouth Junction, NJ, USA) and dissolved in DMSO (Sigma, Saint Louis, USA) at the concentration of 10mM and protected from light. It stored as small aliquots at -20°C for long term preservation. The primers for miR-12315 (HmiRQP4717), miR-1247-3p(HmiRQP3407), miR-33b-3p(HmiRQP0431), miR-320-5p (HmiRQP4731) and small nuclear RNA-U6 (RNU6, #HmiRQP9001) were obtained by Genecopoeia (Rockville, MD, USA). The sequence of miR-12315 inhibitor was: AUGGUGUCGGAAAAUCG UAGCCGAAGACACCUCGGACGA GAGACCGA CACCGCCA. The sequence of miR-1247-3p mimic was: CCCCGGGAACGUCGAGACUGGAGC. The sequence of miR-320a-5p inhibitor was: CGGAAGAGAAGGGCCAAGAAGG. The sequence of miR-33b-3p mimic was:

CAGUGCCU CGGCAGUGCAGCCC. The sequence of inhibitor NC was: CAGUACUUUUGUGUAGUACAA. The sequence of mimic NC was: UUGUACUACACAAAAGUACUG.

*2.2. Cell culture.*

Human cervical cancer cell lines HeLa was purchased from the American Model Culture Collection (ATCC), which was preserved by the State Key Laboratory of Biotherapy of Sichuan University. The cell was cultured in Dulbecco's modified Eagle medium (DMEM) supplemented with 10% fetal bovine serum (FBS; Gibco), 100 unit/mL penicillin( Beyotime, SH, China), and 100 mg/mL streptomycin (Beyotime). These cells were cultured in a humid chamber at 37℃ under 5% CO2 in the atmosphere.

*2.3. Cell viability assay.*

CCK8 kit was used to detect cell proliferation. Briefly, $5x10^3$cells were plated in96 well plates. After attachment overnight, cells were treated with sulforaphane (0, 10, 20, 40μM) for24h, and then incubated in 10% CCK-8 for another 2h. The cells in the 0 μM-treated group were cultured with the same volume of DMSO as the 40μM-treated group. The cell proliferation rate was measured at 450nm absorbance. The experiment was carried out three times.

*2.4. Transcriptome sequencing and analysis.*

HeLa cells were harvested for RNA extraction after 8 h of sulforaphane treatment at a concentration of 40 μM. The cells incubated with the same volume of DMSO as the sulforaphane (40μM)-treated group were set as the control. Each group included three samples. Trizol Reagent (Invitrogen, San Diego, CA, USA) was used to isolate total RNA. Illumina HiSeq 2500 platform was utilized to perform transcriptome sequencing, and 150bp paired-end raw reads were generated. Illumina sequencing was carried out at Novogene, Beijing, China. The expression level of each transcript was measured as the number of clean reads mapped to its reference sequence (GRCh 38). Kallisto[26] was adopted to align and quantify clean reads, genes expressed in at least 1 sample were defined as detected genes. Differential expression analysis was performed through the DEseq2(v 1.24.0) R package [27], DEGs were selected out based on the interval of $p < 0.05$ & $|\log2 \text{ (fold change)}| > 1$. Enrichment of pathways was performed by KOBAS 3.0[28] with the corresponding groups of DEGs. The hypergeometric test method was Fisher's exact test, and the FDR correction method was Benjamini and Hochberg.

*2.5. Small RNA Sequencing and Analysis.*

Small RNAs were sequenced by Illumina Hiseq 2500/2000 platform, and 50 bp single-end reads were generated. Clean data were obtained by removing adaptor sequences, collapsing reads with the same sequence, and reads with less than 15 bases in length from raw data. Then, clean data were analyzed based on the miRDeep2 (2.0.0.8)[29]. Small RNA reads were mapped to miRNA precursors from miRBASE release 22.1[30] by miRDeep2, which allowed zero mismatches. Mapped reads were quantified by miRDeep2. Reads were matched to human miRNA precursors using bowtie2[31], and 1520 miRNAs were detected. Analysis of the differential expressed miRNAs(DEMs) between sulforaphane-untreated and sulforaphane-

treated groups was performed by the DEseq2 R package. $P< 0.05$ & $|\log2 \text{ (fold change)}| > 2$ was set to as the significance threshold in this test. The target genes of DEMs were predicted by TargetScanHuman(v 7.2)[32].The Enrichment of KEGG pathways was performed by KOBAS 3.0 with the target genes.

*2.6. Flowcytometry.*

FITC-Annexin V/PI Detection Kit I (BD Biosciences, San Jose, CA) was used for quantifying the apoptotic cell rate after sulforaphane treatment. The HeLa cells ($5\times10^5$ cells/well) were plated in 6-well plates. After 24 h incubation, the cells were cultured with different concentrations of sulforaphane for 24 h. Then the cells were collected and incubated with Annexin V-FITC for 5 min in the dark and then stained with PI for 5 min. The sample was sorted by NovoCyte flow cytometry. Data were analyzed by NovoExpress 1.1.2 software.

*2.7. miRNA transfection.*

MiR-1247-3p mimic and its scrambled control (NC) were both purchased from GenePharma (Shanghai, China). For transfection, the cells were seeded at a density of $4\times10^4$ cells per well into 6-well culture plates. As the cells reached 50–80 % confluence, transient transfection was performed by using Lipofectamine™ 3000 (Invitrogen) according to the manufactures' protocol. The transfection was stopped after 24 hours, and cells were collected for subsequent experiments, including cell viability and apoptosis assays. In cell viability assay, the cells transfected with different miRNA mimics were administrated with sulforaphane (0, 10, 20, and 40μM) for 24h. In apoptosis assay, the flow cytometry detected the apoptotic cell rate of sulforaphane-treated cells (0, 40μM) for 24h. The cells in the sulforaphane (0 μM)-treated group(control group) were incubated with the same volume of DMSO as the sulforaphane (40 μM)-treated group.

*2.8. Immunofluorescence.*

HeLa cells were seed onto a 14-mm cover glass in 24-well plate and incubated overnight. Cells were treated by different concentrations of sulforaphane for 48h. Then the culture medium was removed, and cells were washed twice with PBS, fixed with 4% paraformaldehyde for 10min and washed three times. The unspecific binding sites were blocked with PBST containing 1% BSA and 0.05% Triton X-100. Subsequently, cells were incubated with primary antibody overnight at 4°C. The secondary antibodies combined with FITC were used. DAPI was performed to stained cell nuclei, and the samples were examined with fluorescence microscopy.

*2.9. RT-PCR.*

To confirm the bioinformatics analysis, total RNA was extracted by using RNA Extraction Kit (TIANGEN BIOTECH, DP419) after treatment with or without sulforaphane (40 μM) for 8 h, and reverse transcribed to cDNA by using Prime Script RT Kit (Takara, RR036) according to the manufacturers' instructions. The qPCR array was performed by using SYBR Select Master Mix (Invitrogen, 4472908) with specific gene primers in StepOnePlus PCR System (Thermo). RT-qPCR was conducted by the following conditions: 95°C for 15 min, followed by 40 cycles of 94°C for 20 s and 60°C for 34 s. RNU6 was used as an internal reference. The target genes expression levels were measured by using the $2^{-\Delta Ct}$ method.

*2.10. Western blot.*

The harvested cells were washed twice with a pre-cooled PBS buffer. Cellular proteins were extracted in RIPA lysis buffer (Biosharp, Guangzhou, GD, China), including protease inhibitor cocktail (Millipore) over ice for 30 minutes. The supernatant was gathered by centrifuging at 13000rpm for 15 min at 4°C. The protein concentrations of samples were evaluated by BCA protein assay kit (Beyotime, China). Afterwards, the protein extracts were separated in SDS-PAGE gel and transferred onto nitrocellulose (NC) membranes (Merck Millipore, MS, USA). Then, the membranes were blocked at room temperature for 1.5h and incubated with proper primary antibody and the corresponding secondary antibody. These primary antibodies were purchased from HuaBio (Hangzhou, ZJ, China), including anti-Cytochrome C antibody (#ET1610-16), anti-Bax antibody (#ET1603-34), anti-β-Actin antibody (#R1207-1). The other primary antibodies were purchased from Cell Signaling Technology, including anti-p-ERK (#4370), anti-ERK(#4695), (anti-p-JNK(#9255), anti –JNK(#9252), anti-p-P38(#4511) and anti -P38(#8690). The specific protein bands were detected via chemiluminescence detection.

*2.11. Statistical analysis.*

All the statistics were carried out in GraphPad Prism 7 and 8. All data are shown as mean ± SD. A two-tailed Student's t-test was used to analyze statistical significance. The statistic differences are shown as * $p < 0.05$, ** p b< 0.01, *** $p < 0.001$, ns, no significance.

## 3. Results and Discussion

*3.1. Sulforaphane inhibited the proliferation and induced apoptosis of HeLa cells.*

To evaluate the effect of sulforaphane on cell viability, the HeLa cell was cultured with sulforaphane of different concentrations (0, 10, 20, 40, and 60μM) for 24 h. According to the results of our CCK-8 array, sulforaphane suppressed the viability of HeLa cells in a concentration-dependent manner (Fig. 1A).

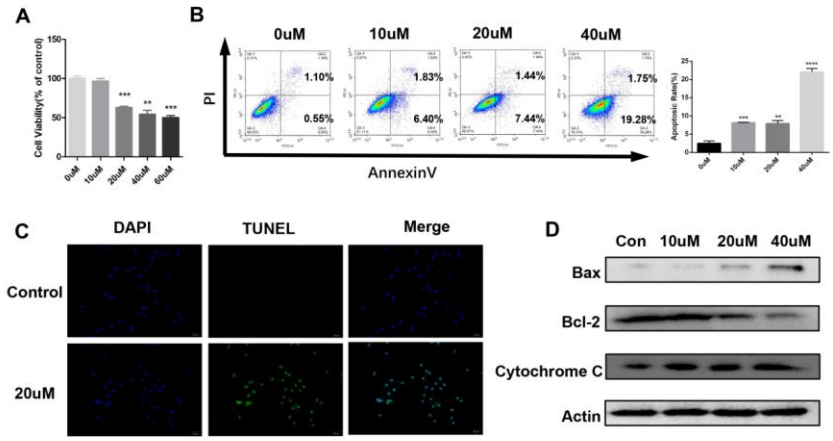


**Figure 1.** Sulforaphane inhibited the proliferation and induced apoptosis of HeLa cells. (**A**) The viability of cells pre-treated with sulforaphane (0, 10, 20, 40, 60μM) was detected. (**B**) Flow cytometric analysis of HeLa cells apoptosis using the Annexin V/PI dual-labeling technique after sulforaphane treatment (0, 10, 20, 40μM)) for 24h. (**C**) Apoptosis of the sulforaphane-treated group and control group were calculated by TUNEL assays. (**D**) Protein level expression of apoptosis in cell pre-treated with 0, 10, 20, and 40μM sulforaphane. Data are shown as mean ± SEM (n=3); * P<0.05, ** P<0.01, *** P<0.001 vs. control group.

As shown in Fig. 1B, the flow cytometry analysis showed the apoptotic rate of HeLa cells of 40μM treatment after 24h remarkably increased compared with the rate of 0μM after 24h. Moreover, the apoptosis rate determined by the TUNEL assay increased (Fig. 1C). To further investigate apoptosis induced by sulforaphane, we analyzed the expression of Bcl-2, Bax, and Cytochrome C. As demonstrated in Fig. 1D, the expression level of anti-apoptotic Bcl-2 decreased. At the same time, pro-apoptotic Bax and Cytochrome C were up-regulated in a dose-dependent manner, which contributed to an increase in the Bax/Bcl-2 expression ratio. All of these proteins were crucial molecular regulators in the mitochondrial-mediated apoptotic pathway [33]. These data indicated that sulforaphane could inhibit the proliferation and induce the apoptosis of HeLa cells.

*3.2. An integrated analysis of altered mRNAs and miRNAs via high-throughput sequencing.*

According to the previous results, transcriptome sequencing and bioinformatics analysis were performed to the HeLa cells treated with sulforaphane at a concentration of 40 μM for 8h. Next-generation sequencing was applied to identify a large number of altered mRNAs and miRNAs after treatment. The analysis of transcription sequencing data described that a total of 21,582 expressed genes were detected.

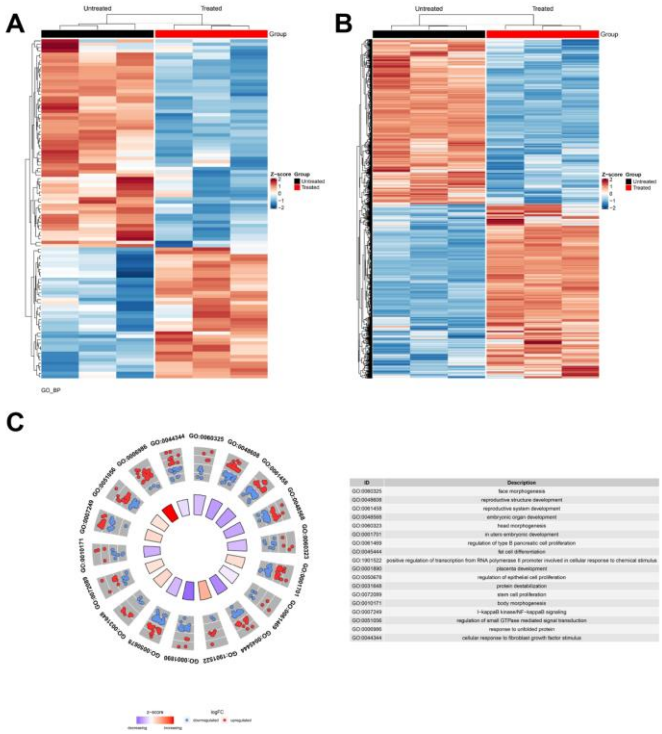


**Figure 2.** High throughputs RNA sequencing of the sulforaphane treatment group and control group. (**A**) Heatmap of the count data of miRNAs that expression changed significantly (P<0.05) in HeLa cells treated with sulforaphane 40uM for 8 hours (n=3). (**B**) Hierarchical clustering heatmap of TPM data of significantly changed genes after sulforaphane treatment. The color density indicates the average expression of a given gene, with each row normalized by z-score. (**C**) GO plot of genes with different expression levels (P < 0.05) of the sulforaphane-treated group in the biological process category of GO enrichment analysis. Red and blue dots in the scatter plot of outer wheel show up-regulated genes and downregulated genes, respectively; the inner wheel demonstrates the z-score.

The expression level of 7838 genes changed significantly (P < 0.05) in the sulforaphane-treated group compared with the control group (Fig 2A). Ultimately, 2041 DEGs were identified by the DEseq2(v 1.24.0) R package. After the analysis of miRNA sequencing data, a total of 1588 miRNAs were spotted. Then the differential expression analysis of these detected miRNAs was performed between the sulforaphane-treated group and the control group

(Fig 2B). Finally, 101 significantly changed miRNAs were found ($P < 0.05$), which contained 39 up-regulated miRNAs and 62 downregulated miRNAs. To better determine the function of DEGs after sulforaphane expose, gene ontology (GO) enrichment analysis was used to find significantly enriched terms, leading to a more comprehensive understanding of the effects sulforaphane exerting on HeLa cells (Fig 2C). The results displayed that many biological processes were significantly altered after sulforaphane treatment, including response to unfolding protein (GO: 0006986), reproductive structure development (GO: 0048608), reproductive system development (G0:0061458), embryonic organ development(GO: 0048568).

### *3.3. Upregulation of miR-1247-3p promoted cell proliferation and induced anti-apoptosis in HeLa cells.*

Several studies suggested that sulforaphane initiated its anti-tumor and anti-inflammatory activities by regulating several miRNAs[23,34-37]. To further explore the role of sulforaphane, we evaluated miRNAs expression via high throughput RNA sequencing. Further, we identified the differential expression level of the miRNAs by the volcano plot in both the control group and the experiment group, as shown in Fig. 3A. Among the four significantly differentially expressed miRNAs, two miRNAs were up-regulated (miR-320a-5p, miR-12135), and the other two miRNAs were downregulated (miR-1247-3p, miR-33b-3p). qPCR was used to confirm the differential miRNA expression.

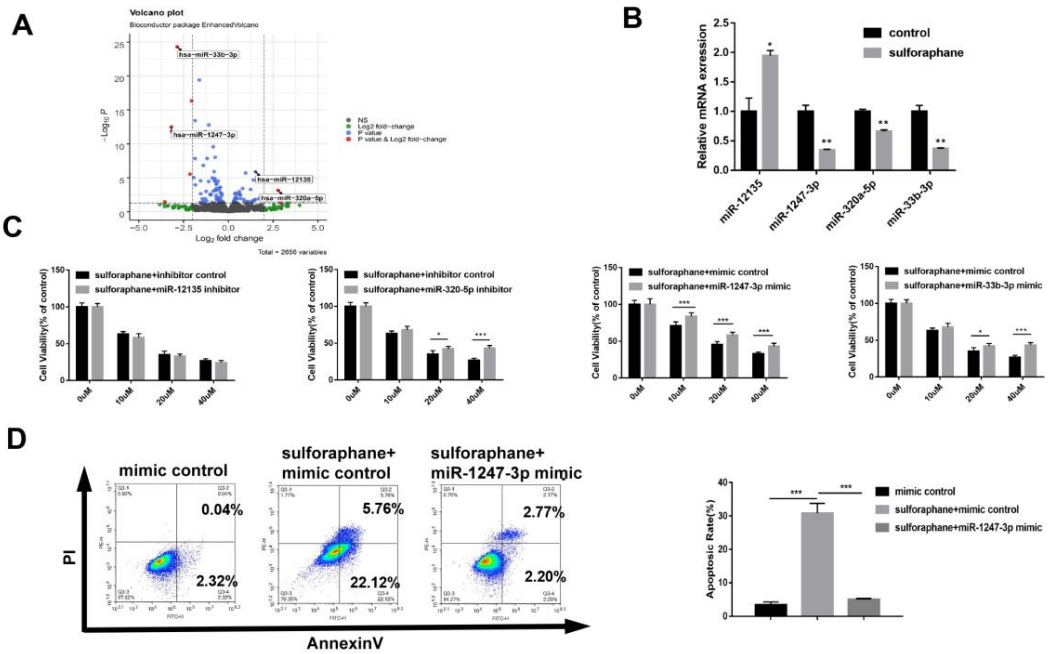


**Figure 3.** MiR-1247-3p was validated to regulate sulforaphane-induced apoptosis in HeLa cells. (**A**) A Volcano plot of miRNA microarray analysis, which was described with the log2 (fold change) of miRNAs expression level and p-value based on −log10. The red dots mean the DEMs based on $p<0.05$ (represented by black horizontal line) and 4-fold expression difference (represented by two black vertical lines), and the top changed four DEMs were labeled. (**B**) Relative miRNA expression in HeLa cells after sulforaphane treatment (40 μM). (**C**) The viability of HeLa cells transfected with top changed four DEMs. (**D**) Flow cytometry analysis of apoptosis rate between the control group and miR-1247-3p transfected group by using the Annexin V/PI dual-labeling technique after 40uM sulforaphane treatment for 24h. Data are shown as mean ± SEM (n=3); * $P < 0.05$, ** $P < 0.01$, *** $P < 0.005$.

The expression of these miRNAs, except for miR-320a-5p, was consistent with RNA-sequencing results (Fig.3B). Next, we tried to examine whether the four miRNAs would impact tumor cell proliferation. The result of the CCK-8 array exhibited that miR-1247-3p mimic could significantly increase HeLa cell proliferation (Fig.3C). Additionally, flow cytometry results confirmed that miR-1247-3p mimic dramatically inhibited cell apoptosis induced by sulforaphane(Fig. 3D). Thus, these results suggested miR-1247-3p could contribute to the anti-apoptotic effect of sulforaphane on HeLa cells.

*3.4. Sulforaphane activated MAPK signaling pathway through downregulating miR-1247-3p.*

To find the mechanism of sulforaphane-induced apoptosis and further investigate the functions of miR-1247-3p, 2725 target genes were obtained (SupplyTable1) to predict the potential target pathways of miR-1247-3p (Fig 4A). Then KEGG pathway analysis was also carried out to explore the signaling pathways of the DEGs between sulforaphane-untreated and treated groups. The top 10 significantly enriched pathways are shown in Fig 4B, and the results are shown in SupplyTable 2. Some studies have revealed that sulforaphane exerted anti-tumor and anti-inflammatory effects via regulating MAPK signaling pathway[38-43].

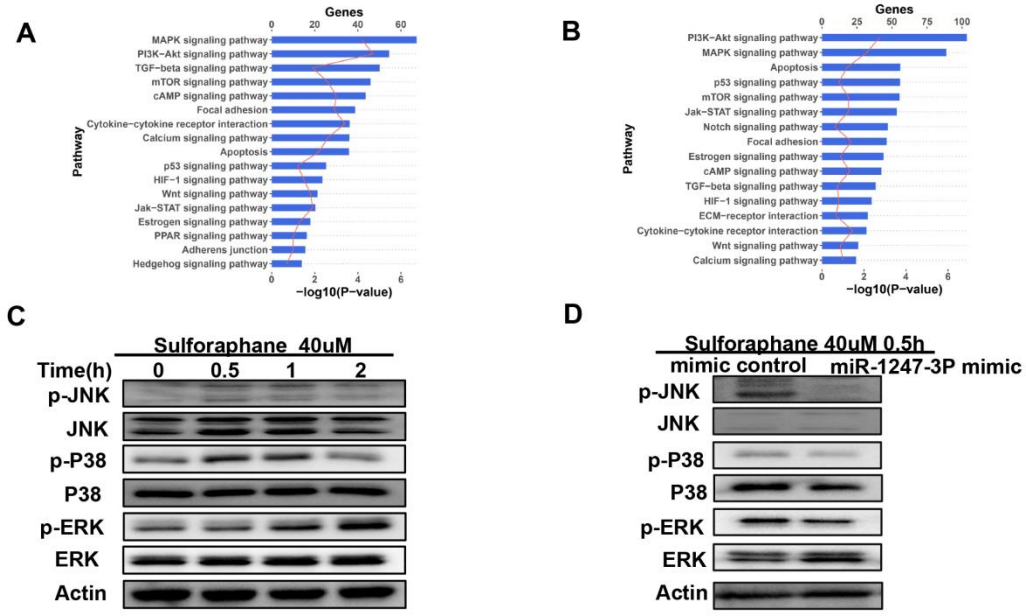


**Figure 4** Sulforaphane activated MAPK signaling pathway via downregulating miR-1247-3p. (**A**) KEGG pathway enrichment analysis for target genes of miR-1247-3p, the top 10 significantly enriched pathways are presented. (**B**) Kyoto Encyclopedia of Genes and Genomes (KEGG) pathway enrichment analysis for DEGs between the sulforaphane treatment group and control group, the top 10 significantly enriched pathways are selected. For each KEGG pathway, the blue bar shows the p-value based on −log10 of the pathway, and the red line present hit genes number. (**C**) Western blot analysis of protein level of MAPK pathway in HeLa cells treated with 40uM of sulforaphane for 0.5 h, 1h, and 2h. Expressions of all the proteins were up-regulated with increasing time. (**D**) Protein expression levels of main factors in MAPK pathway after treatment with sulforaphane with or without miR-1247-3p mimic transfection.

So we tried to examine whether miR-1247-3p was implicated in the regulatory effect of sulforaphane via MAPK pathway on HeLa cells. The results showed that sulforaphane remarkably elevated the phosphorylation levels of JNK, P38, ERK (Fig. 4C). To further confirm these results, we detected JNK, P38, ERK protein levels between the mimic control group and miR-1247-3p mimic group. Results in Fig. 4D showed that the expression of p-JNK,

p-P38, and p-ERK in cells transfected with miR-1247-3P mimic was much lower than that in mimic control-transfected cells. Therefore, these results implied that sulforaphane might downregulate miR-1247-3p to activate MAPK signaling pathway.

## 4. Conclusions

In summary, high throughput sequencing was applied in sulforaphane-treated HeLa cells, and we identified miR1247-3p downregulation was implicated in the pro-apoptosis effect of sulforaphane. Additionally, miR1247-3p-driven MAPK signaling pathway might be attributable to the apoptosis of HeLa cells. Based on the aforementioned mechanism, sulforaphane could serve as a promising anticancer agent in the treatment of cervical cancer.

## Funding

This research received no external funding.

## Acknowledgments

Yunuo Zhao and Dian Fan performed the molecular biology experiments. Meng Luo, Yinan Xiao, and Dingyue Zhang wrote the draft. Hao Zeng performed the miRNA chip analysis. Xuelei Ma designed the research and provided fund support.

## Conflicts of Interest

The authors declare no conflict of interest.

## Data Availability Statement

The raw data of next-generation sequencing used to support the findings of this study are available from the corresponding author upon request.

## References

1. Arbyn, M.; Weiderpass, E.; Bruni, L.; de Sanjose, S.; Saraiya, M.; Ferlay, J.; Bray, F. Estimates of incidence and mortality of cervical cancer in 2018: a worldwide analysis. *Lancet Glob Health* **2020**, *8*, e191-e203, https://doi.org/10.1016/S2214-109X(19)30482-6.
2. Cohen, P.A.; Jhingran, A.; Oaknin, A.; Denny, L. Cervical cancer. *Lancet* **2019**, *393*, 169-182, https://doi.org/10.1016/S0140-6736(18)32470-X.
3. Ferlay, J.; Soerjomataram, I.; Dikshit, R.; Eser, S.; Mathers, C.; Rebelo, M.; Parkin, D.M.; Forman, D.; Bray, F. Cancer incidence and mortality worldwide: sources, methods and major patterns in GLOBOCAN 2012. *Int J Cancer* **2015**, *136*, E359-386, https://doi.org/10.1002/ijc.29210.
4. Sawaya, G.F.; Smith-McCune, K.; Kuppermann, M. Cervical Cancer Screening: More Choices in 2019. *JAMA* **2019**, *321*, 2018-2019, https://doi.org/10.1001/jama.2019.4595.
5. Rachmadi, L.; Siregar, N.C.; Kanoko, M.; Andrijono, A.; Bardosono, S.; Suryandari, D.A.; Sekarutami, S.M.; Hernowo, B.S. Role of Cancer Stem Cell, Apoptotic Factor, DNA Repair, and Telomerase Toward Radiation Therapy Response in Stage IIIB Cervical Cancer. *Oman Med J* **2019**, *34*, 224-230, https://doi.org/10.5001/omj.2019.43.
6. Singh, K.; Connors, S.L.; Macklin, E.A.; Smith, K.D.; Fahey, J.W.; Talalay, P.; Zimmerman, A.W. Sulforaphane treatment of autism spectrum disorder (ASD). *Proc Natl Acad Sci U S A* **2014**, *111*, 15550-15555, https://doi.org/10.1073/pnas.1416940111.
7. Rodova, M.; Fu, J.; Watkins, D.N.; Srivastava, R.K.; Shankar, S. Sonic hedgehog signaling inhibition provides opportunities for targeted therapy by sulforaphane in regulating pancreatic cancer stem cell self-renewal. *PLoS One* **2012**, *7*, https://doi.org/10.1371/journal.pone.0046083.
8. Elkashty, O.A.; Ashry, R.; Elghanam, G.A.; Pham, H.M.; Su, X.; Stegen, C.; Tran, S.D. Broccoli extract improves chemotherapeutic drug efficacy against head-neck squamous cell carcinomas. *Med Oncol* **2018**, *35*, https://doi.org/10.1007/s12032-018-1186-4.

9. Kan, S.F.; Wang, J.; Sun, G.X. Sulforaphane regulates apoptosis- and proliferationrelated signaling pathways and synergizes with cisplatin to suppress human ovarian cancer. *Int J Mol Med* **2018**, *42*, 2447-2458, https://doi.org/10.3892/ijmm.2018.3860.
10. Singh, K.B.; Hahm, E.R.; Alumkal, J.J.; Foley, L.M.; Hitchens, T.K.; Shiva, S.S.; Parikh, R.A.; Jacobs, B.L.; Singh, S.V. Reversal of the Warburg phenomenon in chemoprevention of prostate cancer by sulforaphane. *Carcinogenesis* **2019**, *40*, 1545-1556, https://doi.org/10.1093/carcin/bgz155.
11. Bushati, N.; Cohen, S.M. MicroRNA functions. *Annu Rev Cell Dev Bi* **2007**, *23*, 175-205.
12. Lu, T.X.; Rothenberg, M.E. MicroRNA. *J Allergy Clin Immunol* **2018**, *141*, 1202-1207, https://doi.org/10.1016/j.jaci.2017.08.034.
13. Warde-Farley, D.; Donaldson, S.L.; Comes, O.; Zuberi, K.; Badrawi, R.; Chao, P.; Franz, M.; Grouios, C.; Kazi, F.; Lopes, C.T.; Maitland, A.; Mostafavi, S.; Montojo, J.; Shao, Q.; Wright, G.; Bader, G.D.; Morris, Q. The GeneMANIA prediction server: biological network integration for gene prioritization and predicting gene function. *Nucleic Acids Research* **2010**, *38*, W214-W220, https://doi.org/10.1093/nar/gkq537.
14. Kinser, H.E.; Pincus, Z. MicroRNAs as modulators of longevity and the aging process. *Hum Genet* **2020**, *139*, 291-308, https://doi.org/10.1007/s00439-019-02046-0.
15. Zhou, B.; Zuo, X.X.; Li, Y.S.; Gao, S.M.; Dai, X.D.; Zhu, H.L.; Luo, H. Integration of microRNA and mRNA expression profiles in the skin of systemic sclerosis patients. *Sci Rep-Uk* **2017**, *7*, https://doi.org/10.1038/srep42899.
16. Duttagupta, R.; Jiang, R.; Gollub, J.; Getts, R.C.; Jones, K.W. Impact of Cellular miRNAs on Circulating miRNA Biomarker Signatures. *Plos One* **2011**, *6*, https://doi.org/10.1371/journal.pone.0020769.
17. Gasparello, J.; Gambari, L.; Papi, C.; Rozzi, A.; Manicardi, A.; Corradini, R.; Gambari, R.; Finotti, A. High Levels of Apoptosis Are Induced in the Human Colon Cancer HT-29 Cell Line by Co-Administration of Sulforaphane and a Peptide Nucleic Acid Targeting miR-15b-5p. *Nucleic Acid Ther* **2020**, *30*, 164-174, https://doi.org/10.1089/nat.2019.0825.
18. Gao, L.; Cheng, D.; Yang, J.; Wu, R.; Li, W.; Kong, A.N. Sulforaphane epigenetically demethylates the CpG sites of the miR-9-3 promoter and reactivates miR-9-3 expression in human lung cancer A549 cells. *J Nutr Biochem* **2018**, *56*, 109-115, https://doi.org/10.1016/j.jnutbio.2018.01.015.
19. Kiani, S.; Akhavan-Niaki, H.; Fattahi, S.; Kavoosian, S.; Babaian Jelodar, N.; Bagheri, N.; Najafi Zarrini, H. Purified sulforaphane from broccoli (Brassica oleracea var. italica) leads to alterations of CDX1 and CDX2 expression and changes in miR-9 and miR-326 levels in human gastric cancer cells. *Gene* **2018**, *678*, 115-123, https://doi.org/10.1016/j.gene.2018.08.026.
20. Chen, X.; Jiang, Z.; Zhou, C.; Chen, K.; Li, X.; Wang, Z.; Wu, Z.; Ma, J.; Ma, Q.; Duan, W. Activation of Nrf2 by Sulforaphane Inhibits High Glucose-Induced Progression of Pancreatic Cancer via AMPK Dependent Signaling. *Cell Physiol Biochem* **2018**, *50*, 1201-1215, https://doi.org/10.1159/000494547.
21. Alyoussef, A.; Taha, M. Antitumor activity of sulforaphane in mice model of skin cancer via blocking sulfatase-2. *Exp Dermatol* **2019**, *28*, 28-34, https://doi.org/10.1111/exd.13802.
22. Koolivand, M.; Ansari, M.; Piroozian, F.; Moein, S.; Malek Zadeh, K. Alleviating the progression of acute myeloid leukemia (AML) by sulforaphane through controlling miR-155 levels. *Mol Biol Rep* **2018**, *45*, 2491-2499, https://doi.org/10.1007/s11033-018-4416-0.
23. Li, X.; Zhao, Z.; Li, M.; Liu, M.; Bahena, A.; Zhang, Y.; Zhang, Y.; Nambiar, C.; Liu, G. Sulforaphane promotes apoptosis, and inhibits proliferation and self-renewal of nasopharyngeal cancer cells by targeting STAT signal through miRNA-124-3p. *Biomed Pharmacother* **2018**, *103*, 473-481, https://doi.org/10.1016/j.biopha.2018.03.121.
24. Xia, Y.F.; Pei, G.H.; Wang, N.; Che, Y.C.; Yu, F.S.; Yin, F.F.; Liu, H.X.; Luo, B.; Wang, Y.K. miR-3156-3p is downregulated in HPV-positive cervical cancer and performs as a tumor-suppressive miRNA. *Virol J* **2017**, *14*, 20, https://doi.org/10.1186/s12985-017-0695-7.
25. Hua, F.F.; Liu, S.S.; Zhu, L.H.; Wang, Y.H.; Liang, X.; Ma, N.; Shi, H.R. MiRNA-338-3p regulates cervical cancer cells proliferation by targeting MACC1 through MAPK signaling pathway. *Eur Rev Med Pharmacol Sci* **2017**, *21*, 5342-5352, https://doi.org/10.26355/eurrev_201712_13919.
26. Bray, N.L.; Pimentel, H.; Melsted, P.; Pachter, L. Near-optimal probabilistic RNA-seq quantification. *Nat Biotechnol* **2016**, *34*, 525-527, https://doi.org/10.1038/nbt.3519.
27. Love, M.I.; Huber, W.; Anders, S. Moderated estimation of fold change and dispersion for RNA-seq data with DESeq2. *Genome Biol* **2014**, *15*, 550, https://doi.org/10.1186/s13059-014-0550-8.
28. Ai, C.; Kong, L. CGPS: A machine learning-based approach integrating multiple gene set analysis tools for better prioritization of biologically relevant pathways. *J Genet Genomics* **2018**, *45*, 489-504, https://doi.org/10.1016/j.jgg.2018.08.002.
29. Friedlander, M.R.; Mackowiak, S.D.; Li, N.; Chen, W.; Rajewsky, N. miRDeep2 accurately identifies known and hundreds of novel microRNA genes in seven animal clades. *Nucleic Acids Res* **2012**, *40*, 37-52, https://doi.org/10.1093/nar/gkr688.
30. Kozomara, A.; Birgaoanu, M.; Griffiths-Jones, S. miRBase: from microRNA sequences to function. *Nucleic Acids Res* **2019**, *47*, D155-D162, https://doi.org/10.1093/nar/gky1141.
31. Langmead, B.; Salzberg, S.L. Fast gapped-read alignment with Bowtie 2. *Nat Methods* **2012**, *9*, 357-359, https://doi.org/10.1038/nmeth.1923.

32. Agarwal, V.; Bell, G.W.; Nam, J.W.; Bartel, D.P. Predicting effective microRNA target sites in mammalian mRNAs. *Elife* **2015**, *4*, https://doi.org/10.7554/eLife.05005.
33. Goan, Y.G.; Wu, W.T.; Liu, C.I.; Neoh, C.A.; Wu, Y.J. Involvement of Mitochondrial Dysfunction, Endoplasmic Reticulum Stress, and the PI3K/AKT/mTOR Pathway in Nobiletin-Induced Apoptosis of Human Bladder Cancer Cells. *Molecules* **2019**, *24*, https://doi.org/10.3390/molecules24162881.
34. Lan, F.; Pan, Q.; Yu, H.; Yue, X. Sulforaphane enhances temozolomide-induced apoptosis because of down-regulation of miR-21 via Wnt/beta-catenin signaling in glioblastoma. *J Neurochem* **2015**, *134*, 811-818, https://doi.org/10.1111/jnc.13174.
35. Eren, E.; Tufekci, K.U.; Isci, K.B.; Tastan, B.; Genc, K.; Genc, S. Sulforaphane Inhibits Lipopolysaccharide-Induced Inflammation, Cytotoxicity, Oxidative Stress, and miR-155 Expression and Switches to Mox Phenotype through Activating Extracellular Signal-Regulated Kinase 1/2-Nuclear Factor Erythroid 2-Related Factor 2/Antioxidant Response Element Pathway in Murine Microglial Cells. *Front Immunol* **2018**, *9*, https://doi.org/10.3389/fimmu.2018.00036.
36. An, Y.W.; Jhang, K.A.; Woo, S.Y.; Kang, J.L.; Chong, Y.H. Sulforaphane exerts its anti-inflammatory effect against amyloid-beta peptide via STAT-1 dephosphorylation and activation of Nrf2/HO-1 cascade in human THP-1 macrophages. *Neurobiol Aging* **2016**, *38*, 1-10, https://doi.org/10.1016/j.neurobiolaging.2015.10.016.
37. Wang, D.X.; Zou, Y.J.; Zhuang, X.B.; Chen, S.X.; Lin, Y.; Li, W.L.; Lin, J.J.; Lin, Z.Q. Sulforaphane suppresses EMT and metastasis in human lung cancer through miR-616-5p-mediated GSK3beta/beta-catenin signaling pathways. *Acta Pharmacol Sin* **2017**, *38*, 241-251, https://doi.org/10.1038/aps.2016.122.
38. Reddy, S.A.; Shelar, S.B.; Dang, T.M.; Lee, B.N.; Yang, H.; Ong, S.M.; Ng, H.L.; Chui, W.K.; Wong, S.C.; Chew, E.H. Sulforaphane and its methylcarbonyl analogs inhibit the LPS-stimulated inflammatory response in human monocytes through modulating cytokine production, suppressing chemotactic migration and phagocytosis in a NF-kappaB- and MAPK-dependent manner. *Int Immunopharmacol* **2015**, *24*, 440-450, https://doi.org/10.1016/j.intimp.2014.12.037.
39. Shan, Y.; Wang, X.; Wang, W.; He, C.; Bao, Y. p38 MAPK plays a distinct role in sulforaphane-induced up-regulation of ARE-dependent enzymes and down-regulation of COX-2 in human bladder cancer cells. *Oncol Rep* **2010**, *23*, 1133-1138, https://doi.org/10.3892/or_00000742.
40. Ren, J.; Yuan, L.; Wang, Y.; Chen, G.; Hu, K. Benzyl sulforaphane is superior to sulforaphane in inhibiting the Akt/MAPK and activating the Nrf2/ARE signalling pathways in HepG2 cells. *J Pharm Pharmacol* **2018**, *70*, 1643-1653, https://doi.org/10.1111/jphp.13015.
41. Qin, S.; Yang, C.; Huang, W.; Du, S.; Mai, H.; Xiao, J.; Lu, T. Sulforaphane attenuates microglia-mediated neuronal necroptosis through down-regulation of MAPK/NF-kappaB signaling pathways in LPS-activated BV-2 microglia. *Pharmacol Res* **2018**, *133*, 218-235, https://doi.org/10.1016/j.phrs.2018.01.014.
42. Mondal, A.; Biswas, R.; Rhee, Y.H.; Kim, J.; Ahn, J.C. Sulforaphene promotes Bax/Bcl2, MAPK-dependent human gastric cancer AGS cells apoptosis and inhibits migration via EGFR, p-ERK1/2 down-regulation. *Gen Physiol Biophys* **2016**, *35*, 25-34.
43. Kim, B.G.; Fujita, T.; Stankovic, K.M.; Welling, D.B.; Moon, I.S.; Choi, J.Y.; Yun, J.; Kang, J.S.; Lee, J.D. Sulforaphane, a natural component of broccoli, inhibits vestibular schwannoma growth in vitro and in vivo. *Sci Rep* **2016**, *6*, 36215, https://doi.org/10.1038/srep36215.

# Supplementary files

## SupplyTable 1

| Target | SFRP5 | ARL5C |
|---|---|---|
| BOK | TBXA2R | MCF2L2 |
| CXCR3 | HMBS | VSTM4 |
| SHOX | KIAA0513 | BARHL1 |
| CRX | MEX3B | WDR20 |
| KCTD17 | PRX | AC140061.12 |
| SLC25A34 | MARVELD1 | RP11-297N6.4 |
| DLX2 | AOAH | NXF1 |
| C1QTNF6 | HSH2D | KCNE3 |
| SELM | SYVN1 | FAM63B |
| PNMA6C | SLC39A3 | TBC1D22A |
| PNMA6A | LY6G5B | DUSP22 |
| SMIM7 | TUSC5 | MFAP3 |
| AL590822.2 | IL31 | HOXC5 |
| LTBP4 | HIC1 | LRTM2 |
| AGXT | PSME3 | GREM2 |
| PHLDB3 | TCL1A | MICU1 |
| C17orf103 | REM1 | HTR4 |
| GNLY | OTUD6A | CHRM1 |
| ALKBH4 | TSSK6 | NDUFS7 |
| TMUB1 | RNF125 | RP11-644F5.10 |
| TECPR1 | C17orf107 | RAX2 |
| CCL17 | C10orf105 | TMSB10 |
| SPEF1 | IER5L | EFCAB4A |
| TOR4A | C3orf80 | AL591479.1 |
| AC115618.1 | STX4 | C11orf96 |
| FOXA3 | CASP16 | C2orf88 |
| B4GALT3 | USP11 | C19orf33 |
| CEP72 | PTGES2 | AAED1 |
| NDP | MGAT5B | ADM |
| SERPINF2 | STAT5A | ZNF70 |
| C15orf62 | VPS37B | EVX2 |
| ORAI2 | PPP1R27 | AP3S2 |
| PTPRN2 | LHFPL5 | ZNF835 |
| IL25 | SCNN1G | CTB-102L5.4 |
| TREML1 | CSNK2B-LY6G5B-1181 | CASP2 |
| LUC7L | DDX11 | HABP4 |
| FLJ00104 | TMEM95 | BHLHA9 |
| AC025278.1 | NEU1 | LRRN4CL |
| TRPV2 | IL23R | PAX2 |
| RP11-863K10.7 | DIDO1 | ARMS2 |
| TUBB2B | DZANK1 | NYAP1 |
| GNB1L | RP11-834C11.12 | CNNM4 |
| ARHGDIG | PDDC1 | CYP4F2 |
| ANKS6 | AC006967.1 | ANGPTL2 |
| ZMAT3 | GPR108 | NMNAT1 |
| PTGES | C19orf25 | RP11-831H9.11 |
| GOSR2 | SYT5 | C11orf48 |
| MAP4 | HAGHL | FBLIM1 |
| AC000003.2 | SMPD3 | FAM169B |
| PLCXD1 | POU3F1 | ACAD10 |
| CTXN1 | CTD-2054N24.2 | MARK2 |
| CACNG4 | ALDH1A3 | PCDH1 |
| UTS2R | GAB4 | VHLL |
| BTBD19 | GJD3 | DPYSL5 |
| PNMA3 | VAV1 | RP11-131H24.4 |
| C13orf35 | SIX2 | CCDC81 |

| | | |
|---|---|---|
| ABHD17B | CDKL1 | SSTR1 |
| GDPD1 | A4GALT | LSM4 |
| CHST13 | TLE6 | PRDM12 |
| C6orf226 | AC021860.1 | C8orf31 |
| INPP5D | MIF | IKBKG |
| CARD14 | CRKL | PITPNM3 |
| WBSCR16 | ZNF154 | ESM1 |
| TXNRD1 | CXorf56 | SSTR5 |
| LRRC1 | CTRC | PEPD |
| GPR75 | KIF14 | FAM213A |
| SCARF1 | ZFPL1 | FOXB1 |
| ENGASE | OVGP1 | C1orf229 |
| ADRB1 | TPM1 | FOXN1 |
| LRFN1 | XPNPEP2 | FAM53C |
| AGPAT2 | SGSM1 | FAM83C |
| MDM4 | OAZ3 | RABAC1 |
| PARP10 | GSG2 | NAT8L |
| RASD2 | CREB3L3 | PRRG3 |
| STAT1 | C14orf182 | CERS1 |
| KCNK13 | AC140481.2 | BIRC5 |
| SFTPC | MRFAP1 | SH2D3A |
| AJAP1 | PPARD | DNAJA3 |
| ZNF454 | MFI2 | DMRTA2 |
| LCNL1 | IGHMBP2 | IGF2 |
| POU4F1 | PAOX | CLUH |
| ULK3 | ZNF106 | FRAT2 |
| C15orf38-AP3S2 | TRIM8 | FEV |
| B3GAT3 | Z98049.1 | FECH |
| WFDC8 | ZNF791 | UBE2L3 |
| PSAPL1 | LRRC3DN | SBK1 |
| KLHL17 | SP140L | DNAJB1 |
| L2HGDH | FOXC2 | BTBD11 |
| SLC6A1 | CHST6 | PEX26 |
| SLC30A7 | CD209 | SNPH |
| FOXD2 | SOCS2 | AL626787.1 |
| ATXN7L3 | FAM9B | ATG9B |
| DHRS4 | GTF2IRD1 | U2AF1L4 |
| FAM84A | MRPL28 | TBC1D13 |
| ZNF430 | MOGS | AP000350.10 |
| RASA3 | SYK | GJA5 |
| GLRA4 | TBC1D28 | TRMT112 |
| ZBTB8A | HCLS1 | ZFAND4 |
| IFITM5 | C1orf159 | C1QTNF4 |
| CPZ | RRP7A | AC004899.1 |
| CLPS | AP005482.1 | UPF1 |
| TIMM44 | PSMG4 | STX16 |
| IVD | EIF4EBP2 | DNAJC5 |
| PRKAB1 | ALPI | ZNF213 |
| KCNIP3 | NR1I3 | ALAD |
| NFIX | TAF8 | TMEM259 |
| MDM2 | OGG1 | AL645728.1 |
| TXNRD2 | SOWAHD | FEZF1 |
| MTRNR2L4 | AMER3 | NUDC |
| SLC52A3 | CPT1A | PRKAR1B |
| ZNF234 | FADS6 | LAX1 |
| AC009892.10 | RP11-93B14.6 | DLGAP2 |
| USP36 | AFMID | SLC18A1 |
| FOXK1 | GRK1 | LRRC3 |
| MRPL55 | DIRAS1 | SULT1A1 |
| CELF5 | VWA1 | KIAA0754 |
| GABPB2 | TACSTD2 | HOXB6 |
| PTK6 | CBX6 | ZBTB7C |

| COL4A5 |
|---|
| AC006486.1 |
| SLC39A11 |
| POM121L7 |
| SMARCD3 |
| SYT15 |
| CCM2L |
| TMEM107 |
| AL359091.2 |
| GATA2 |
| STPG1 |
| ELF3 |
| SNCB |
| NTSR1 |
| KCNAB3 |
| ARIH2OS |
| NWD1 |
| RTN4RL1 |
| TARS2 |
| MED6 |
| AC005003.1 |
| FBXL18 |
| HAGH |
| AL020996.1 |
| TMEM145 |
| NLRP12 |
| LINC00908 |
| FAHD1 |
| MLC1 |
| TEN1 |
| FAIM2 |
| ING5 |
| MPV17L |
| MUL1 |
| SIGLEC11 |
| C14orf23 |
| MCAT |
| KCNH6 |
| GNB2 |
| RNASEK |
| C2orf48 |
| SLC44A4 |
| VMO1 |
| CCL5 |
| PLEKHA4 |
| TPD52L2 |
| TSPO |
| CDK10 |
| MAGEB10 |
| CTB-167G5.5 |
| PPID |
| AL357673.1 |
| CTA-299D3.8 |
| CASP3 |
| DPH7 |
| NTRK2 |
| MTHFSD |
| ADCK4 |
| ROGDI |
| APCDD1L |
| SNAI1 |
| AC022532.1 |

| WNT7B |
|---|
| TNFSF10 |
| CTSD |
| C12orf68 |
| FAM60A |
| DAND5 |
| CALML6 |
| FAM76A |
| TOMM40 |
| C5AR2 |
| AC016722.1 |
| TMEM132E |
| CPLX2 |
| LYZ |
| SYNDIG1 |
| CXCL14 |
| HM13 |
| FAM86A |
| CACNB1 |
| RCAN1 |
| KALRN |
| GINS4 |
| NCR3LG1 |
| FAM110D |
| BLOC1S3 |
| STAU1 |
| APOBEC3A |
| CEACAM5 |
| CD300E |
| OSCAR |
| CAMK1D |
| METTL8 |
| FAM78A |
| SPTBN2 |
| PIGW |
| NKX6-3 |
| CYB561 |
| OSBPL2 |
| FAM156B |
| SCRT1 |
| FAM156A |
| CHMP6 |
| RPH3AL |
| SLC39A13 |
| SLC9A1 |
| ALDH18A1 |
| CDC14B |
| DNAJC14 |
| GPR35 |
| ARHGAP19-SLIT1 |
| SCN5A |
| C5orf45 |
| ADAMTS4 |
| COPG1 |
| SLC14A2 |
| HIST1H2AG |
| ZNF175 |
| C4orf26 |
| ZNF157 |
| HPCAL1 |
| ZGLP1 |
| NEK8 |

| CELF6 |
|---|
| NUBP2 |
| XYLT2 |
| EN1 |
| AMBP |
| SERF1A |
| SERF1B |
| AC016559.1 |
| FANCC |
| DAB2IP |
| GGA3 |
| DDX51 |
| SCRT2 |
| FCRLB |
| ARSK |
| PIM1 |
| CD300C |
| ZBTB47 |
| URAD |
| CHRNB1 |
| GLTP |
| RAB40C |
| WIZ |
| CEACAM18 |
| GDPD5 |
| KANK2 |
| SFMBT2 |
| SLC35E3 |
| NT5C1A |
| NRTN |
| RBM7 |
| CIC |
| C19orf40 |
| RADIL |
| MX1 |
| TNNT2 |
| CARD10 |
| SERBP1 |
| AC105020.1 |
| NHSL1 |
| LRRC27 |
| ST8SIA2 |
| RBM3 |
| ANKRD40 |
| TRPM2 |
| EPN3 |
| FAM64A |
| LOH12CR2 |
| NCS1 |
| AC079210.1 |
| ALDH3B1 |
| ENSG00000270466 |
| SGTA |
| NSMF |
| ZNF773 |
| PHYHD1 |
| NKX2-5 |
| NAT9 |
| RPS15A |
| PAK4 |
| WFDC1 |
| NDNL2 |

| FDX1L |
|---|
| ENTPD6 |
| NELFB |
| RSL1D1 |
| TRAPPC2 |
| TRIM54 |
| WIPI1 |
| FGFR4 |
| PPP1R3G |
| PIPOX |
| KIAA1257 |
| PPP1R8 |
| CARM1 |
| NAALADL1 |
| ICAM4 |
| MBOAT1 |
| NR1H2 |
| PRKX |
| EXTL1 |
| FFAR2 |
| LGI3 |
| LAIR1 |
| UBE2G2 |
| TLR10 |
| APOL2 |
| PRDM8 |
| TAF13 |
| LRRC14B |
| EFNA2 |
| FLJ30594 |
| COX7B |
| LYRM2 |
| NFIC |
| DUX4L2 |
| TUBB6 |
| OSM |
| P4HB |
| ELMOD1 |
| ARF5 |
| AC112693.2 |
| ANO10 |
| CRCP |
| TMED4 |
| ADRBK1 |
| ARL6IP1 |
| APITD1-CORT |
| C9orf66 |
| CTD-2162K18.4 |
| INPPL1 |
| ASCL5 |
| ANKRD36 |
| GJA9 |
| NICN1 |
| ZFP42 |
| TUBA3D |
| ID3 |
| ZBP1 |
| GTPBP3 |
| CTD-2368P22.1 |
| TWF2 |
| FAM86B1 |
| DDX31 |

| ATP13A1 |
|---|
| NRXN2 |
| METTL7A |
| NBEAL2 |
| TNFRSF1B |
| KCTD5 |
| RETSAT |
| KLHL30 |
| SOBP |
| TMCO3 |
| ATP6V1B1 |
| FBLN5 |
| C7orf43 |
| MYO3A |
| MKNK2 |
| SLC2A6 |
| P2RX7 |
| H1F0 |
| NRIP3 |
| CYTH4 |
| C10orf55 |
| TNFSF14 |
| CDK5R2 |
| C2orf15 |
| MRPL30 |
| CASC10 |
| COQ10B |
| SPC24 |
| SYNGR1 |
| SNRPB |
| TBC1D32 |
| PTX4 |
| HAND1 |
| TBCCD1 |
| TAF1 |
| RAB8A |
| RRP1B |
| IFFO1 |
| UBXN2A |
| MLX |
| ECSIT |
| ZNF143 |
| LYSMD1 |
| CA13 |
| IL10RB |
| TAB1 |
| INPP5E |
| NANOG |
| FRMD1 |
| FAM219A |
| EFHD2 |
| RICTOR |
| QRFPR |
| ATPIF1 |
| NTM |
| LPCAT2 |
| UST |
| IL21R |
| TCF7 |
| BAIAP2L1 |
| ZNF512B |
| ARMC5 |

| FOXM1 |
|---|
| VASH1 |
| PPP2R1A |
| RFNG |
| TMEM106A |
| ACOT4 |
| CENPH |
| RNF222 |
| GCM1 |
| DUSP13 |
| KREMEN1 |
| CHST8 |
| ULBP3 |
| TCHP |
| ARHGAP40 |
| DLST |
| TMEM150C |
| TLR7 |
| VSIG8 |
| AL161915.1 |
| TBX4 |
| NRG1 |
| NUTM2E |
| ATP2A3 |
| KCNMB1 |
| TRPV1 |
| SHPK |
| ZCCHC4 |
| ARHGEF18 |
| TSGA13 |
| SYT3 |
| ATG4B |
| TULP1 |
| PRKAB2 |
| BIVM |
| ATMIN |
| CECR1 |
| AP3B2 |
| GAS2L1 |
| SLMO1 |
| CXCR2 |
| SLC25A15 |
| JAKMIP3 |
| RNF44 |
| C4orf40 |
| MEN1 |
| PALM |
| DPP9 |
| EBI3 |
| MARVELD2 |
| PI4K2A |
| TMEM130 |
| PTCHD2 |
| HOXB4 |
| WNT3A |
| ZNF827 |
| VPS53 |
| PPP6R1 |
| COLQ |
| CCDC18 |
| C5orf64 |
| PRSS38 |

| XKR8 |
|---|
| ALG1 |
| AL450307.1 |
| MLLT4 |
| CIB2 |
| RIOK3 |
| KBTBD6 |
| PIM2 |
| SLC7A14 |
| POLH |
| AKT1S1 |
| C8orf82 |
| TOR2A |
| USP24 |
| RNF224 |
| RWDD2A |
| ACOT9 |
| SLC2A3 |
| VGF |
| SPDEF |
| FAM53A |
| EVC |
| CTDSP2 |
| PARD6G |
| SIRT6 |
| TGIF2 |
| HMG20A |
| GRK7 |
| MAPK8IP3 |
| CYP51A1 |
| ZNF383 |
| PSTPIP2 |
| PRRG2 |
| TECPR2 |
| RP11-1118M6.1 |
| FLNB |
| AC137932.1 |
| RAET1E |
| LMOD3 |
| AC084121.16 |
| MS4A7 |
| PYGB |
| MRTO4 |
| BPNT1 |
| AC104841.2 |
| KRT15 |
| ECT2L |
| C1orf111 |
| KCNF1 |
| DUSP18 |
| TSNARE1 |
| TAF1D |
| RAB3B |
| STK40 |
| CD82 |
| MYO3B |
| ZNF362 |
| CALM3 |
| MINOS1 |
| CLSTN1 |
| NHLH1 |
| SYNE2 |

| H6PD |
|---|
| LCN6 |
| ZBTB8OS |
| ICOSLG |
| TNFAIP3 |
| HIST2H3C |
| NCK2 |
| HIST2H3A |
| MYO1C |
| ADM2 |
| GDNF |
| SNAPC2 |
| TMEM105 |
| ZNF697 |
| PODXL2 |
| HSPA6 |
| ZNF556 |
| RAB3D |
| ABCB8 |
| HIST1H2BF |
| BSG |
| C21orf2 |
| FAM20C |
| ARFRP1 |
| WDR92 |
| ZBTB39 |
| RINL |
| C19orf35 |
| SCAMP5 |
| ZNF492 |
| ZNF44 |
| SLC16A13 |
| MAVS |
| POU4F3 |
| ZNF91 |
| STAC2 |
| DAPP1 |
| SLC25A32 |
| PARD6B |
| FBXL22 |
| EXD1 |
| PIWIL2 |
| KCNT1 |
| 1-Mar |
| PDE6G |
| OR7D2 |
| PDE4C |
| AC093157.1 |
| KRT6B |
| SLC29A4 |
| HCAR1 |
| C2orf50 |
| WDR5B |
| MOCOS |
| ANKRD29 |
| THAP5 |
| PARD3B |
| HAPLN4 |
| CASKIN1 |
| VHL |
| ECE1 |
| GCAT |

| ST3GAL2 |
|---|
| PTBP1 |
| BRSK1 |
| AC135983.2 |
| WFIKKN2 |
| BHLHA15 |
| PBX1 |
| ZBTB25 |
| C8orf44-SGK3 |
| CRTC1 |
| ZNF385A |
| NDE1 |
| KLC1 |
| SOX18 |
| C6orf123 |
| RBBP9 |
| LTB4R |
| THEMIS2 |
| NOTO |
| CYP8B1 |
| ZNF573 |
| ZFR2 |
| MBD3 |
| ARHGAP39 |
| CEP104 |
| NRARP |
| RBM43 |
| FAM9C |
| AC011484.1 |
| ASB1 |
| PTGDR2 |
| LDOC1 |
| ABHD12 |
| AMPD2 |
| MKS1 |
| ZNF557 |
| FGF22 |
| SMIM14 |
| PARP11 |
| NUBPL |
| SLC28A1 |
| ZNF878 |
| IFNAR1 |
| SHH |
| CDC25B |
| CCDC137 |
| EGR3 |
| LPGAT1 |
| ANKRD62 |
| FAM132A |
| PGP |
| CCDC117 |
| SNAI3 |
| SVOP |
| PHYHIP |
| CCRN4L |
| ZIM3 |
| MALL |
| TRMT2B |
| NIPAL2 |
| PLD3 |
| PPFIA3 |

| ZNF665 |
| --- |
| HTR1D |
| RD3 |
| TP53 |
| PHF20 |
| STK11 |
| TSPYL1 |
| DTX3L |
| POM121 |
| WBP2 |
| ZFYVE26 |
| SSBP3 |
| CX3CL1 |
| TAF1L |
| NR2F6 |
| SPI1 |
| ESCO2 |
| PMM2 |
| RBM48 |
| ARSD |
| LL22NC03-63E9.3 |
| ZNF587B |
| SCARA3 |
| SGK3 |
| HRH1 |
| SOST |
| VWA3A |
| AC145676.2 |
| KCNJ15 |
| C21orf90 |
| PSMB11 |
| YPEL2 |
| NOS1AP |
| TNFAIP2 |
| ANKRD63 |
| PHF21B |
| MFSD7 |
| NAPA |
| NUAK2 |
| PAICS |
| POLR2D |
| RPH3A |
| ATAD3C |
| RPS21 |
| TLCD2 |
| HRH4 |
| TNK2 |
| LAMP2 |
| OTOF |
| AC079612.1 |
| KCNK6 |
| TRAFD1 |
| ZNF813 |
| ACVRL1 |
| KCNK5 |
| OLFML2A |
| ALG12 |
| GPR82 |
| GSX1 |
| SLC35B4 |
| GPR176 |
| ZNF528 |

| GINM1 |
| --- |
| RIPPLY3 |
| NFATC2IP |
| VIPR1 |
| DUX4L5 |
| C22orf46 |
| FOXJ3 |
| MAPK14 |
| GATC |
| FAM173A |
| SNX22 |
| LAMP3 |
| SUN2 |
| SLC26A4 |
| TNNT3 |
| RGS9BP |
| KEAP1 |
| RDH13 |
| CLEC16A |
| FAM19A5 |
| SEMA7A |
| PDLIM5 |
| CES4A |
| GJB1 |
| FUT1 |
| ERAP2 |
| FOXQ1 |
| ZNF101 |
| AQP2 |
| OPA3 |
| POU2F2 |
| DUX4 |
| MYO16 |
| DUX4L3 |
| DUX4L7 |
| DUX4L4 |
| LHX3 |
| ITGAX |
| DUX4L6 |
| ADCY9 |
| MYOD1 |
| LILRB3 |
| FAM217B |
| EREG |
| RFX1 |
| PRR26 |
| USP54 |
| ZNF793 |
| VEGFA |
| MBP |
| INMT |
| C6orf223 |
| SURF6 |
| PITX1 |
| AC006372.1 |
| HLA-E |
| MPL |
| KRT86 |
| CDH4 |
| ARX |
| AL021546.6 |
| DOK7 |

| APOL4 |
| --- |
| PM20D1 |
| GAS2L3 |
| MYADM |
| BCL2L2 |
| CBX7 |
| BEGAIN |
| DNAAF3 |
| CCDC85B |
| ADAP1 |
| ZNF554 |
| WTIP |
| PLAT |
| CCNJ |
| MRPS17 |
| RAD23A |
| ZBTB42 |
| SAE1 |
| AC008132.1 |
| DSG3 |
| S1PR2 |
| TOR1AIP1 |
| ICMT |
| ZNF726 |
| TNFRSF11A |
| OMP |
| ATP6V1A |
| AMBRA1 |
| KANK4 |
| TNRC6C |
| LDLR |
| SERINC5 |
| FAM73A |
| ACACB |
| NAIP |
| ZNF749 |
| GBP2 |
| TFAP4 |
| PPIP5K1 |
| SERPINB9 |
| AP000350.4 |
| MAPK11 |
| MAFG |
| ZFP90 |
| PTPLB |
| RASAL1 |
| KLHL6 |
| NRF1 |
| NCCRP1 |
| GMPS |
| SOX1 |
| SLC11A1 |
| OR2C3 |
| GNL3L |
| HIST1H3F |
| SCN2B |
| ATP2B3 |
| SYNPO |
| STX2 |
| C11orf70 |
| IL2RB |
| PAX5 |

| SCARF2 |
|---|
| RNF34 |
| CASP8 |
| CRISPLD2 |
| IGFN1 |
| 9-Sep |
| IRF5 |
| CA12 |
| FAM213B |
| SMARCD1 |
| SCD5 |
| PGBD4 |
| PHF7 |
| CCDC40 |
| NUDT4 |
| PITPNM2 |
| GMEB2 |
| ISLR2 |
| SLC46A1 |
| NAGPA |
| ACVR1B |
| OTUD3 |
| ANKS3 |
| HIF1AN |
| DENR |
| FKTN |
| TCF21 |
| FGD2 |
| HSPB6 |
| UNC5B |
| PIAS4 |
| HRAS |
| DCAF16 |
| DHDDS |
| ZNF2 |
| DCP1A |
| TMEM236 |
| TMEM236 |
| SLC7A6 |
| SLIT1 |
| IL17RE |
| MFSD2B |
| FUT3 |
| FZD7 |
| SFXN5 |
| ZNF418 |
| OTUD5 |
| FICD |
| COL27A1 |
| MFN1 |
| SPRYD3 |
| TAL2 |
| NCLN |
| RPL36 |
| MCMDC2 |
| ACSS1 |
| TSTA3 |
| RPS6KB1 |
| STK32A |
| PRKAA1 |
| IKZF4 |
| ACTRT3 |

| PSMB2 |
|---|
| LIPH |
| WDR55 |
| NPAS4 |
| KCNC1 |
| GLTPD1 |
| ZSCAN22 |
| SP1 |
| PHKA2 |
| MGAT3 |
| GNE |
| TRIM35 |
| UBN2 |
| KIAA1147 |
| ABCF3 |
| NUP155 |
| CST3 |
| C14orf132 |
| FKBP14 |
| RNF4 |
| THAP6 |
| MCC |
| FSD2 |
| CACNA1C |
| KIAA1919 |
| ITGB3 |
| BRCA1 |
| GPR116 |
| TEF |
| FLG2 |
| MINOS1-NBL1 |
| PRELP |
| SRRM4 |
| GPR144 |
| ZNF695 |
| ZNF397 |
| EFNA3 |
| MTL5 |
| ICA1L |
| MCCC2 |
| FEM1A |
| ZNF618 |
| NKX3-2 |
| CTSF |
| TERF2 |
| MAP2K4 |
| UTP11L |
| GRINA |
| KNOP1 |
| SYTL4 |
| ZNF543 |
| TAS2R5 |
| ARMC10 |
| CASZ1 |
| ZNF669 |
| LPIN3 |
| NR1I2 |
| FAM83H |
| IL11 |
| ARID3A |
| SPPL2A |
| GRIN3A |

| STK17B |
|---|
| FGFRL1 |
| MPLKIP |
| NBL1 |
| DGKQ |
| MAFA |
| THRA |
| INSR |
| VMA21 |
| ARIH1 |
| SGTB |
| NIPAL1 |
| ZNF562 |
| STK25 |
| SERTAD2 |
| ZC3HAV1 |
| GPR56 |
| TTL |
| S1PR3 |
| IMPDH1 |
| FBXO27 |
| TMEM170A |
| UBE2W |
| UBA2 |
| BCKDK |
| NARF |
| DUSP19 |
| RPUSD1 |
| SMYD4 |
| SLX4 |
| FRRS1L |
| CLNK |
| NOM1 |
| CHRNA4 |
| PPARA |
| ZFP36L1 |
| HOXD3 |
| C19orf54 |
| YPEL1 |
| DSG2 |
| DSTYK |
| TNFRSF8 |
| EXOSC10 |
| SP9 |
| KLHL21 |
| DCTN3 |
| CD96 |
| AP1S3 |
| AKIP1 |
| CTU1 |
| OTUD7B |
| PPM1F |
| RARG |
| SLC9A5 |
| MIEF1 |
| SMIM19 |
| KRT83 |
| AZGP1 |
| SLC12A5 |
| LOH12CR1 |
| ITPRIPL2 |
| TMEM184B |

| SLC12A3 |
| --- |
| GPR123 |
| KIAA0930 |
| SPOCD1 |
| SPN |
| ASB16 |
| PHACTR2 |
| B3GALNT2 |
| CHL1 |
| LRRC10B |
| KIAA1614 |
| DENND6B |
| ZNF487 |
| SP8 |
| TAPBP |
| AC019294.1 |
| LLGL2 |
| AIRE |
| TXNDC15 |
| SP110 |
| OCLN |
| WWP2 |
| ITPK1 |
| ELOVL3 |
| PACSIN2 |
| FAM227A |
| LRRC58 |
| YIPF4 |
| GIT2 |
| FBXO46 |
| CLSPN |
| FSCN1 |
| SFRP1 |
| POM121C |
| APLN |
| RNF144A |
| C1orf170 |
| MR1 |
| TMEM127 |
| LRP10 |
| AGMAT |
| ZNF740 |
| GNB5 |
| BRI3BP |
| CDKN2B |
| FAM160B2 |
| TSPEAR |
| RASGRF1 |
| ELAVL1 |
| HIST1H3E |
| USP20 |
| LEPROT |
| MGRN1 |
| HK2 |
| GPR37L1 |
| SLC16A8 |
| CLCN2 |
| LYRM7 |
| GRAMD4 |
| SEMA6C |
| C2CD4C |
| DDR1 |

| NAIF1 |
| --- |
| ITGA11 |
| AKNA |
| SEC22C |
| IRGQ |
| CDC42EP1 |
| HOXB3 |
| GIPR |
| CEMP1 |
| RAB11FIP3 |
| HOOK3 |
| FAM222B |
| OPRL1 |
| TMEM109 |
| COX6B2 |
| SLC26A2 |
| SGMS2 |
| PIK3C2B |
| CSPG4 |
| ASIC4 |
| TTLL12 |
| ATF7IP |
| MACC1 |
| PPP1R12B |
| GRK5 |
| FOPNL |
| TOX4 |
| ZNF850 |
| QPCTL |
| NPAS1 |
| DYNC1LI2 |
| MIEF2 |
| AVL9 |
| ST5 |
| SYT7 |
| C4orf29 |
| MITF |
| FBXO45 |
| UNC5A |
| TBX20 |
| C2orf71 |
| TPCN1 |
| FBXO31 |
| KCNE4 |
| NECAB3 |
| C1RL |
| KAT7 |
| FAM212B |
| ZRANB3 |
| MYO1D |
| ADAMTS13 |
| SH3PXD2A |
| RBBP4 |
| TNFRSF25 |
| NKPD1 |
| STON2 |
| IFNLR1 |
| HEPACAM |
| FAM43B |
| UMODL1 |
| CR1 |
| C20orf144 |

| DDIT4 |
| --- |
| PAX8 |
| ITGA2 |
| BAI2 |
| CCDC71L |
| FAT2 |
| NBEAL1 |
| NEURL1B |
| CLCN7 |
| RTCA |
| PNPLA3 |
| RP5-850E9.3 |
| TRABD2B |
| GPSM1 |
| LRRC32 |
| DENND6A |
| CELSR1 |
| TRPM4 |
| ZNF451 |
| FOXO1 |
| SPATA5 |
| SCN4B |
| NLRC3 |
| NT5DC3 |
| CSNK1G2 |
| STS |
| LIX1L |
| NFKBID |
| TMEM55B |
| CD72 |
| RAN |
| KIAA0355 |
| BBC3 |
| ITPKC |
| SKOR1 |
| SRXN1 |
| TIA1 |
| RNF157 |
| GLG1 |
| GPRC5B |
| SPRED3 |
| SNX11 |
| S100B |
| TRPV3 |
| RFX2 |
| C1orf106 |
| KAZALD1 |
| COL5A1 |
| F11R |
| C19orf55 |
| DDX49 |
| FOXL1 |
| ATXN3 |
| SRGAP1 |
| LRRD1 |
| SYNRG |
| MLLT3 |
| EVX1 |
| BTD |
| ZBED1 |
| LRIG2 |
| STEAP2 |

| ZFYVE20 |
|---|
| RARA |
| RUNX3 |
| INTU |
| ZNF816 |
| GNPNAT1 |
| TRUB2 |
| KIAA0825 |
| UNC13A |
| NOL9 |
| GSTK1 |
| ZNF621 |
| CENPI |
| PGAM5 |
| CACNA1A |
| RNF114 |
| EPS8L2 |
| CD3EAP |
| GRM6 |
| STRA6 |
| FRMD4A |
| CPNE5 |
| REEP3 |
| SOX12 |
| CCDC127 |
| N4BP1 |
| ACTR1A |
| RAPGEF1 |
| CARD8 |
| ZNF710 |
| UBOX5 |
| NEUROG3 |
| CEP135 |
| ZNF629 |
| ATAD5 |
| ZMYM1 |
| CEBPD |
| SLC9A3R2 |
| HAP1 |
| ZNF460 |
| COX19 |
| C17orf51 |
| ZNF207 |
| MLLT1 |
| REXO1 |
| NTN1 |
| RPUSD4 |
| PDCL3 |
| TRAF3IP2 |
| RAD23B |
| ZNF264 |
| UHRF1BP1 |
| GBX2 |
| ITFG3 |
| CACNA1I |
| TMEM104 |
| SLC7A1 |
| CHMP1B |
| PADI2 |
| RPS6KA2 |
| PACS1 |
| NPY4R |

| RNF7 |
|---|
| CNNM3 |
| DSC3 |
| SLC12A6 |
| PEX13 |
| PGPEP1 |
| RUFY3 |
| STK4 |
| PHLDA3 |
| SLC43A2 |
| SRPX2 |
| FAM163A |
| TSPAN11 |
| ZDBF2 |
| NOP9 |
| NDOR1 |
| SPNS2 |
| HK1 |
| ELFN2 |
| C2CD2L |
| TH |
| SH3GL1 |
| PLEKHG4B |
| ACSF3 |
| SLC35A3 |
| KIF26A |
| ATCAY |
| NARFL |
| ATP6V1C2 |
| PCDHB11 |
| MLXIP |
| PLCH2 |
| PLA2G6 |
| ELK4 |
| KCNJ6 |
| KCNAB2 |
| KIAA1456 |
| NKX6-2 |
| SRM |
| DPPA3 |
| TONSL |
| HSD17B13 |
| MPRIP |
| HIC2 |
| AC021218.2 |
| MYO9B |
| AL049840.1 |
| NXN |
| PEX2 |
| ELL |
| ZNF155 |
| RABL5 |
| PLEKHA6 |
| ZNF805 |
| TMEM184A |
| IKBIP |
| DRAXIN |
| CBX2 |
| MTMR9 |
| KIAA1210 |
| TLN2 |
| PTPN14 |

| LSM11 |
|---|
| HIST1H2BD |
| SLC35F6 |
| HRK |
| RGS3 |
| CD3G |
| CAPN15 |
| NRG2 |
| ESPN |
| SMAD9 |
| PPP2R3B |
| LPP |
| LEPREL1 |
| BMPR1A |
| JUND |
| BSPRY |
| NMT1 |
| SYTL3 |
| TPPP |
| NPTX1 |
| ITGB8 |
| HAUS3 |
| WDR31 |
| ZNF85 |
| DUSP2 |
| STRIP2 |
| SF3B5 |
| DNMT3A |
| FBXL16 |
| LAMC3 |
| MAP3K9 |
| FBXL2 |
| PHF15 |
| ZNF587 |
| SBSPON |
| WDR70 |
| AGAP1 |
| LPHN1 |
| H2AFV |
| CCDC142 |
| KCNK3 |
| HGFAC |
| ZNF841 |
| PRKCB |
| SLC25A29 |
| TMEM255B |
| C9orf69 |
| EVI5 |
| GDF11 |
| NR6A1 |
| PODXL |
| MINK1 |
| SLC22A23 |
| LRCH4 |
| ACOX1 |
| GLRX3 |
| HIST1H2BO |
| DESI1 |
| AGPAT3 |
| AKAP13 |
| TERT |
| SLC33A1 |

| LIMK1 |
|---|
| PLEKHM2 |
| PPARGC1B |
| DNAJC3 |
| XKR4 |
| PLXNB1 |
| TGFBR2 |
| MIOX |
| YY1 |
| EXOSC2 |
| ZNF730 |
| PHAX |
| ACAN |
| DIP2C |
| WNK2 |
| EXOC8 |
| GLYR1 |
| RPP25 |
| XIAP |
| SDK1 |
| DGKE |
| ATG12 |
| TMEM192 |
| SMC5 |
| CLN8 |
| AGPAT6 |
| HMX3 |
| PDP2 |
| ZNF442 |
| KCTD20 |
| KLHL11 |
| DHODH |
| SOX4 |
| GREB1 |
| LSM14A |
| ZER1 |
| MED9 |
| FZD3 |
| IGF2R |
| RCAN3 |
| RASSF6 |
| TBRG1 |
| UQCC1 |
| SIT1 |
| BCAR1 |
| PAPOLG |
| TFAP2B |
| ATP5S |
| ADAMTS17 |
| CANT1 |
| OSTM1 |
| SFXN1 |
| TEX22 |
| OTUD7A |
| GCLM |
| SGPP2 |
| AGAP2 |
| MCM8 |
| ANO7 |
| VKORC1L1 |
| ZNRF3 |
| ZNF551 |

| ISM2 |
|---|
| AP5B1 |
| LDLRAD2 |
| RC3H1 |
| SGSM3 |
| RNASEH2C |
| KCNQ4 |
| MUC20 |
| RASSF2 |
| C3orf36 |
| TMEM120B |
| CSNK1A1 |
| GXYLT2 |
| SRD5A1 |
| FAM131A |
| GNA11 |
| HMX2 |
| AP1G1 |
| ZNF738 |
| IL17RD |
| FOXE1 |
| SNAP29 |
| ANKRD33B |
| MED13L |
| ADAM19 |
| KIF21B |
| SAPCD2 |
| SERINC3 |
| QSOX1 |
| FBXO48 |
| FGD4 |
| SIRT5 |
| ARHGEF15 |
| FBXO10 |
| VENTX |
| VWA5B1 |
| HSPG2 |
| DGCR2 |
| MYLK3 |
| ZNF585B |
| DGKD |
| LRCH3 |
| ZNF696 |
| PTPRS |
| COL8A2 |
| HECTD3 |
| ATP5G1 |
| NDUFA7 |
| IKZF3 |
| SLC12A7 |
| DYM |
| SDF4 |
| RAD1 |
| IMPAD1 |
| TRAPPC2P1 |
| BNIP2 |
| MANEAL |
| GRM1 |
| THSD4 |
| WDR12 |
| TNFRSF14 |
| ABHD15 |

| ARPC2 |
|---|
| METTL21A |
| ISL2 |
| FAM211A |
| LURAP1 |
| HELLS |
| VIPR2 |
| TRIM67 |
| SHISA7 |
| C6orf141 |
| CDC42BPG |
| TIMM8A |
| PLBD2 |
| RUNX1 |
| IQSEC1 |
| ZNF431 |
| SELRC1 |
| AC007040.11 |
| SNIP1 |
| SIM2 |
| APBA1 |
| RNF165 |
| FTO |
| HMGB1 |
| PLXDC1 |
| INHBB |
| IRAK3 |
| ZNF19 |
| PER1 |
| TNFRSF13C |
| HELB |
| ANKRD45 |
| TNPO2 |
| KCNC3 |
| IQCE |
| ATG13 |
| C21orf59 |
| ZNF283 |
| TTC9C |
| CLDN19 |
| SGCB |
| IREB2 |
| HSPA4L |
| PPP6R3 |
| TRIM59 |
| CBX5 |
| CERS4 |
| TNS4 |
| HIPK2 |
| PLEKHG5 |
| RNF126 |
| RIMS3 |
| AC018755.1 |
| TBC1D24 |
| SLC15A2 |
| APBA2 |
| KIAA2018 |
| CYB5R3 |
| FRMPD4 |
| SLC25A1 |
| LRRC47 |
| PLIN5 |

| GLDN |
|---|
| CPLX1 |
| AGTRAP |
| EPHA10 |
| ZC3H8 |
| NOVA2 |
| LONRF2 |
| TMX4 |
| TBC1D16 |
| ZBTB20 |
| PHACTR4 |
| PHACTR1 |
| PANK4 |
| ZDHHC3 |
| ZNF799 |
| PPM1K |
| AP5S1 |
| C4orf33 |
| ONECUT3 |
| HOXD11 |
| ZBTB3 |
| EXPH5 |
| SH3BP2 |
| HDLBP |
| COL9A2 |
| ZDHHC24 |
| PPP1R16B |
| AAK1 |
| PRICKLE1 |
| CENPN |
| NONO |
| RPL18A |
| EHBP1L1 |
| GNB4 |
| CAMK4 |
| BCORL1 |
| HSPA5 |
| FBXL20 |
| DCP2 |
| TRPM6 |
| MOB4 |
| SLC9A7 |
| LMTK2 |
| GDF7 |
| SZT2 |
| AMDHD2 |
| ZNF546 |
| P2RY2 |
| DARS2 |
| ENOSF1 |
| FCF1 |
| MAGI1 |
| SPIRE2 |
| METTL16 |
| GK5 |
| LRRK1 |
| GAS7 |
| UTP6 |
| EIF3L |
| ZNF35 |
| BPTF |
| C12orf5 |

| PVR |
|---|
| MYH9 |
| KLF16 |
| SP6 |
| CMKLR1 |
| CENPP |
| NOL10 |
| IGF1R |
| HIST3H2BB |
| GCNT4 |
| HS3ST1 |
| FAM83F |
| CAPZB |
| C17orf75 |
| PAFAH1B1 |
| RANBP3 |
| FASTKD2 |
| MNT |
| MMS22L |
| ARSG |
| CLCN5 |
| MPPE1 |
| PRSS21 |
| MAGI3 |
| PDK3 |
| C19orf52 |
| KLHDC10 |
| COLGALT2 |
| CAMSAP1 |
| C15orf38 |
| RWDD1 |
| GMPPB |
| THAP1 |
| TRAF6 |
| RXRA |
| RPTOR |
| RAB10 |
| NUP205 |
| UGGT1 |
| USH1G |
| CLMN |
| TSHZ2 |
| EFR3B |
| UTP15 |
| COPA |
| MTUS2 |
| NEUROD2 |
| HSD17B12 |
| KLHL24 |
| KCND3 |
| PPIL6 |
| RAB11FIP4 |
| ZFP30 |
| RBM28 |
| TNRC6B |
| POU2F1 |
| DCPS |
| SEMA3E |
| TRIP11 |
| VPS13B |
| NTNG2 |
| GPR153 |

| PTCD1 |
|---|
| RRP12 |
| WDR91 |
| ZNF566 |
| LRRC28 |
| SIPA1L3 |
| XRCC3 |
| FN3KRP |
| ZNF394 |
| HIST1H2BG |
| CXorf23 |
| HSPE1-MOB4 |
| VMAC |
| C10orf54 |
| VPS13D |
| CPM |
| ZNF419 |
| PLEKHG2 |
| PTBP2 |
| VPS33A |
| GNAL |
| SP5 |
| MTPAP |
| SFT2D2 |
| CENPC |
| MAP2K3 |
| CSPP1 |
| PMPCA |
| SARM1 |
| POLM |
| SYAP1 |
| HMHA1 |
| TENM3 |
| ZFP82 |
| METTL12 |
| GRK4 |
| GATAD2B |
| DNAL1 |
| CDK9 |
| TMEM151A |
| TIAF1 |
| GRIK3 |
| SLC25A16 |
| CHD5 |
| AMD1 |
| BMPR2 |
| ZNF701 |
| FKBP9 |
| ANXA6 |
| RILPL1 |
| GPT2 |
| TMEM168 |
| DUSP28 |
| MICA |
| B3GALT1 |
| KIN |
| TFDP2 |
| SSH3 |
| DOCK11 |
| ATF6 |
| HOMEZ |
| GNPTAB |

| SMS |
|---|
| EHD2 |
| SIAE |
| SLC4A8 |
| ZNF347 |
| AGO3 |
| SLC25A36 |
| ZSCAN29 |
| SLC2A5 |
| PIGQ |
| HHIP |
| POTEM |
| POTEG |
| BRCC3 |
| NEDD4L |
| FAM162A |
| YIPF2 |
| NCAM1 |
| LHFPL4 |
| ZNF446 |
| TANC2 |
| SLC7A11 |
| PLXNA1 |
| NPR1 |
| LPAR3 |
| C15orf40 |
| TOPBP1 |
| SDHAF1 |
| ZNF708 |
| ZSWIM7 |
| CCDC93 |
| ANAPC16 |
| OGFOD3 |
| CIAO1 |
| MEX3A |
| MYO18A |
| LHX1 |
| ARHGAP27 |
| CLUAP1 |
| MAP1LC3B |
| SUMO2 |
| TCEANC2 |
| SMAD4 |
| ABHD2 |
| MKI67IP |
| RNF41 |
| GNG7 |
| GDAP1L1 |
| TMEM220 |
| TMEM186 |
| INPP5K |
| KLHL4 |
| TTC4 |
| NTRK3 |
| NFRKB |
| GTF3C6 |
| USP13 |
| GEMIN6 |
| FASN |
| SNRPD1 |
| CLSTN2 |
| CLPB |

| BDH1 |
|---|
| SUSD1 |
| TPCN2 |
| ZSCAN2 |
| SF3B1 |
| MYCBP |
| KIAA1551 |
| WBSCR27 |
| CELSR2 |
| ZNF766 |
| SWSAP1 |
| GNAI3 |
| ZNF324B |
| PLXNA3 |
| IBA57 |
| HABP2 |
| URM1 |
| NETO2 |
| LETM1 |
| TBRG4 |
| SNCA |
| RBBP8 |
| SERPINA4 |
| FKRP |
| POLR1C |
| ADH5 |
| B4GALT7 |
| RSBN1L |
| TAOK1 |
| PDE12 |
| GABRB3 |
| PHC3 |
| C19orf47 |
| MTMR10 |
| PURB |
| ZHX3 |
| GGCX |
| ZNF790 |
| TIMM50 |
| NFE2L1 |
| IL18BP |
| LANCL3 |
| CD248 |
| SHB |
| E2F3 |
| ARHGAP35 |
| EPHA8 |
| ANKRD13B |
| ANK1 |
| FLJ27365 |
| ERN1 |
| ALPK3 |
| NAV2 |
| C20orf194 |
| GALNT10 |
| GTF2F1 |
| PSKH1 |
| RPL14 |
| CC2D1B |
| LIG3 |
| TSPAN14 |
| ANGEL2 |

| RPL24 |
|---|
| MESDC2 |
| SMU1 |
| ZSCAN16 |
| LATS1 |
| SNRPD3 |
| SH3PXD2B |
| MRPS30 |
| PTPN2 |
| CFD |
| KIAA0101 |
| ANKRD9 |
| IMPA2 |
| PIAS2 |
| DPY19L1 |
| ERGIC2 |
| ANKMY1 |
| GTPBP10 |
| SHPK |
| APPBP2 |
| TMED7 |
| FAM179A |
| PTPRJ |
| PLAGL2 |
| BID |
| MAPK9 |
| DRG1 |
| NACC2 |
| CCDC77 |
| MAP2K6 |
| THEM4 |
| EMB |
| PDZD8 |
| SUMO1 |
| MRPL48 |
| RNF19B |
| VCL |
| PQLC2 |
| MGA |
| CTSB |
| NDUFS1 |
| RSU1 |
| SPRYD7 |
| CCBE1 |
| ARRB1 |
| ZZEF1 |
| ELP3 |
| ABR |
| EHD1 |
| WISP2 |
| TTC39A |
| PTPDC1 |
| TSPAN31 |
| CA5B |
| ORC1 |
| F10 |
| ARSA |
| SLFN12 |
| RAP1A |
| HOXB13 |
| ZNF639 |
| ADARB1 |

| TSKU |
|---|
| ADHFE1 |
| MYPN |
| GADD45GIP1 |
| IRF1 |
| ALDH6A1 |
| NDUFC1 |
| ELP6 |
| SOCS7 |
| LAYN |
| ST3GAL6 |
| CEP68 |
| TLE3 |
| PTCHD1 |
| SOD2 |
| FANCA |
| CDK4 |
| LIMS1 |
| SLC16A10 |
| SCIN |
| C7orf55-LUC7L2 |
| RAB13 |
| SLC1A5 |
| MGP |
| HJURP |
| CDH6 |
| ATP5F1 |
| C17orf85 |
| HLX |
| MON2 |
| AGTPBP1 |
| ADRBK2 |
| RBM4B |
| ABCF1 |
| DDX19B |
| SIRT3 |
| SARDH |
| EMC7 |
| SBNO1 |
| CNKSR3 |
| DNAJC21 |
| C1orf21 |
| SDCCAG3 |
| SORCS2 |
| SLC35F5 |
| NUP43 |
| NAGS |
| NXPE3 |
| ABHD6 |
| BZW1 |
| PRIM1 |
| AQR |
| IMP4 |
| ETFDH |
| LUC7L2 |
| XPNPEP3 |
| AK1 |
| ZNF445 |
| TXNL4A |
| SLC38A9 |
| GPR133 |
| PDE7A |

| FOXRED2 |
|---|
| TGS1 |
| SOX11 |
| CHSY3 |
| GSR |
| NDUFA4 |
| POLR3B |
| CCSER2 |
| NADSYN1 |
| MED28 |
| NABP1 |
| ZNF259 |
| PCM1 |
| GTPBP4 |
| LPAR2 |
| RPP14 |
| PRR24 |
| VPS18 |
| RP1-170O19.20 |
| TTF2 |
| SMAD2 |
| FAM83D |
| HOXA9 |
| F2RL1 |
| APOA1 |
| SIK2 |
| ODF2L |
| PPM1D |
| NME1-NME2 |
| FLYWCH2 |
| C5orf55 |
| HSDL2 |
| CENPM |
| AGXT2 |
| ABCG8 |
| MAML2 |
| MRPS14 |
| CLYBL |
| GTDC1 |
| FANCM |
| ATG2B |
| C14orf80 |
| NME2 |
| ZNF177 |
| TXNL1 |
| P4HA2 |
| PSD4 |
| ABCG2 |
| USP1 |
| APOPT1 |
| CTSV |
| ATP6V0E1 |
| FGFR1OP |
| PYCR1 |
| NNMT |
| CALCOCO2 |
| MTHFR |
| PLAC8 |
| MPI |
| SLC35C2 |
| PHB2 |
| NDUFV3 |

| DNA2 |
|---|
| MRGPRF |
| ASH2L |
| ALG9 |
| GMPR |
| CNBP |
| ALG14 |
| PFAS |
| AP3M1 |
| SCARB2 |
| SOGA3 |
| PCNP |
| RBM15B |
| CDX2 |
| TENM4 |
| CABLES1 |
| POLR2E |
| PGK1 |
| RFFL |
| SMURF1 |
| XPO5 |
| RRAGD |
| OCIAD2 |
| C7orf55 |
| DNLZ |
| FHL2 |
| PELP1 |
| TIFA |
| C21orf58 |
| ACO1 |
| MTDH |
| GLA |
| SIRPA |
| URGCP |
| ALKBH1 |
| MGAT1 |
| DCAF10 |
| MON1B |
| DNAJB5 |
| HIST1H1C |
| TEAD3 |
| MMS19 |
| ZNF559 |
| C3 |
| UBR4 |
| IWS1 |
| RAB40B |
| MRPL17 |
| GLI4 |
| STX1B |
| FADS1 |
| ZNF526 |
| EMILIN2 |
| CHAF1B |
| CKAP2L |
| RFC2 |
| RNF40 |
| ZFAND5 |
| MSANTD4 |
| ZNF107 |
| ZADH2 |
| KNSTRN |

| | | |
|---|---|---|
| VGLL3 | PCDHB2 | BAG2 |
| SRSF9 | GPRIN3 | AP5Z1 |
| TBC1D15 | TMEM135 | MCTS1 |
| NSUN3 | HTT | TMEM179 |
| IPO9 | CORO7 | GPR34 |
| PTGR2 | PPIL2 | ANP32E |
| TIGD2 | DOCK7 | UGGT2 |
| COMTD1 | TM4SF5 | STX7 |
| COPS3 | RASSF4 | TAF1B |
| CKAP4 | DR1 | NIF3L1 |
| CEP63 | KCMF1 | HSPB3 |
| LMF1 | ITGA1 | RPL13 |
| RMDN1 | MAPK8IP2 | PANK2 |
| SELK | MRPS23 | ZNF843 |
| AIG1 | ANKLE2 | AKR7A2 |
| FYTTD1 | GLP2R | RPL23 |
| CHSY1 | ARFIP2 | CLEC4C |
| SSBP2 | EIF4E | LRG1 |
| YME1L1 | CYB5D1 | SLC22A18AS |
| RRM2 | TTC13 | GTF2H5 |
| KB-1507C5.2 | TMEM134 | ABI2 |
| INO80 | ACTR10 | KLHL36 |
| SNAPC3 | ATP6V1E1 | DEFB105B |
| HINFP | LMAN2L | PSMC4 |
| RAD51L3-RFFL | MED16 | CCS |
| RBFA | PRCD | ZNF423 |
| ZNF668 | DBNL | LETMD1 |
| HMGB2 | METTL22 | C3orf83 |
| SLC8A1 | MTHFD1 | PIGP |
| HAS2 | NINJ1 | DEFB105A |
| DSN1 | CYB5R4 | CACNG1 |
| TOP3A | AGT | CCL24 |
| SHOC2 | TFCP2 | ISY1 |
| C16orf72 | MMP15 | GTF2H4 |
| TTC38 | CAND1 | AVPI1 |
| PAN2 | MAPK1 | POLE |
| RNF24 | ZMYM4 | UBP1 |
| C4orf32 | DNAJC10 | SF3A1 |
| SGOL1 | CDS2 | IGSF6 |
| NTMT1 | RPL37A | PLAA |
| ECHDC3 | PRPS1 | ERCC1 |
| PRPF6 | FNDC3B | ALOX15 |
| RELT | AC106017.1 | PNRC1 |
| CMBL | NEK9 | FAM83E |
| FBXO3 | TMEM106B | RBM25 |
| TMEM86B | RNF115 | KY |
| SKP1 | G3BP2 | NCF1 |
| ZNF607 | POLA2 | ERVV-1 |
| CADM1 | GRWD1 | CHID1 |
| SERPING1 | DCUN1D5 | COX16 |
| LYRM4 | DYRK1B | IL17RA |
| MTO1 | RNMTL1 | UBASH3A |
| TRIOBP | SERPINH1 | SAMD15 |
| EMC2 | TNPO1 | ZNF611 |
| NCKAP1 | WDR88 | AKR1D1 |
| SLBP | LDHA | FPR2 |
| DNAJC30 | TIMM10 | CABP4 |
| ENAH | CAPZA2 | TTPA |
| SLC30A5 | ORMDL2 | CLPP |
| DDI2 | DNTTIP2 | BSND |
| NUPL2 | NLN | PTAFR |
| SCO1 | CHD7 | CD300LB |

| IL12RB2 |
| --- |
| MYOZ2 |
| LUC7L3 |
| CDNF |
| RBM23 |
| LHPP |
| HIF1A |
| CD84 |
| CD226 |
| C10orf71 |
| FPR1 |
| FHL5 |
| PRPF4 |
| MBD5 |
| ACOT2 |
| TLK2 |
| AGAP9 |
| GABRR2 |
| GRAP2 |
| CRIPT |
| DDX4 |
| PPIL4 |
| AKAP1 |
| RANBP3L |
| NCL |
| MYBPC1 |
| ATIC |
| TRA2B |
| ABCB11 |
| GLTSCR2 |
| SLFN12L |
| EPHX2 |
| FDFT1 |
| GPR78 |
| SPATS2L |
| BTLA |
| SLC22A12 |
| YIF1B |
| GRM4 |
| MAMDC4 |
| SND1 |
| KLHDC8A |
| ABCA6 |
| TIMM23 |
| SLC24A4 |
| CRP |

| TG |
| --- |
| EMG1 |
| NLRP9 |
| ASB6 |
| AC135178.1 |
| TIMD4 |
| SRSF3 |
| CD3D |
| NDUFB5 |
| C9orf3 |
| MTMR8 |
| ZNF417 |
| SHC3 |
| MYO1F |
| SEMA4F |
| RBP4 |
| TRIM72 |
| SLC16A3 |
| BCDIN3D |
| ATP5J2-PTCD1 |
| EMC1 |
| SMTNL2 |
| SPTLC3 |
| PARP2 |
| ZFP36L2 |
| SLC22A15 |
| RCN2 |
| SSTR2 |
| UQCR11 |
| GPI |
| ZNF8 |
| SELPLG |
| NRXN3 |
| ALOX5AP |
| ALDOA |
| UBC |
| C1orf210 |
| BRIP1 |
| PRMT7 |
| TFB1M |
| MTFMT |
| PRR11 |
| PSMB9 |
| DNAH17 |
| C18orf32 |
| CPNE2 |

| CCNO |
| --- |
| VASN |
| KLF2 |
| CAPRIN1 |
| RLIM |
| CYP20A1 |
| NKD2 |
| NAA50 |
| ANKFY1 |
| FOSL2 |
| TRIM38 |
| SRSF1 |
| NQO2 |
| S100A16 |
| MXRA8 |
| PPAP2B |
| CCNT1 |
| NUP93 |
| KIF1C |
| MSRB2 |
| ATP5G3 |
| ST20-MTHFS |
| STRADA |
| ZNF326 |
| PEX16 |
| POLD4 |
| WDR13 |
| HEYL |
| C1QTNF8 |
| ZNF426 |
| PLA2G16 |
| RIMKLA |
| PPDPF |
| 6-Mar |
| MTHFS |
| SC5D |
| USP4 |
| HSPA1B |
| VCAM1 |
| MRPL15 |
| XBP1 |
| KIAA0408 |
| ARRDC2 |
| GM2A |
| OSTF1 |

# SupplyTable 2

| ##Databases: KEGG PATHWAY |
|---|
| ##Statistical test method: hypergeometric test / Fisher's exact test |
| ##FDR correction method: Benjamini and Hochberg |

| #Term | ID | Input number | Background number | P-Value | Corrected P-Value |
|---|---|---|---|---|---|
| Pathways in cancer | hsa05200 | 50 | 397 | 1.25E-09 | 2.33E-08 |
| Rap1 signaling pathway | hsa04015 | 32 | 211 | 2.64E-08 | 4.24E-07 |
| PI3K-Akt signaling pathway | hsa04151 | 41 | 342 | 1.25E-07 | 1.85E-06 |
| Ras signaling pathway | hsa04014 | 31 | 228 | 3.78E-07 | 5.17E-06 |
| Transcriptional misregulation in cancer | hsa05202 | 27 | 180 | 3.8E-07 | 5.19E-06 |
| Neuroactive ligand-receptor interaction | hsa04080 | 34 | 278 | 9.6E-07 | 1.21E-05 |
| MAPK signaling pathway | hsa04010 | 32 | 255 | 1.2E-06 | 1.49E-05 |
| Signaling pathways regulating pluripotency of stem cells | hsa04550 | 22 | 142 | 2.76E-06 | 3.18E-05 |
| Regulation of actin cytoskeleton | hsa04810 | 28 | 215 | 2.87E-06 | 3.29E-05 |
| Metabolic pathways | hsa01100 | 94 | 1243 | 3.62E-06 | 4.06E-05 |
| TNF signaling pathway | hsa04668 | 17 | 110 | 3.71E-05 | 0.000338 |
| FoxO signaling pathway | hsa04068 | 19 | 134 | 3.86E-05 | 0.000348 |
| Renal cell carcinoma | hsa05211 | 13 | 67 | 3.9E-05 | 0.000351 |
| Glycine serine and threonine metabolism | hsa00260 | 10 | 40 | 4.87E-05 | 0.000432 |
| Influenza A | hsa05164 | 22 | 176 | 5.56E-05 | 0.000485 |
| Longevity regulating pathway - multiple species | hsa04213 | 12 | 64 | 0.000102 | 0.000834 |
| Insulin resistance | hsa04931 | 16 | 109 | 0.000107 | 0.000868 |
| Measles | hsa05162 | 18 | 136 | 0.000134 | 0.001052 |
| Apoptosis | hsa04210 | 18 | 140 | 0.000186 | 0.001392 |
| p53 signaling pathway | hsa04115 | 12 | 69 | 0.000191 | 0.00142 |
| mTOR signaling pathway | hsa04150 | 19 | 154 | 0.000202 | 0.001497 |
| Circadian rhythm | hsa04710 | 8 | 31 | 0.00023 | 0.001674 |
| beta-Alanine metabolism | hsa00410 | 8 | 31 | 0.00023 | 0.001674 |
| Longevity regulating pathway | hsa04211 | 14 | 94 | 0.000247 | 0.001783 |
| Jak-STAT signaling pathway | hsa04630 | 19 | 158 | 0.000271 | 0.001926 |
| Endocytosis | hsa04144 | 26 | 260 | 0.000344 | 0.002355 |
| Axon guidance | hsa04360 | 20 | 176 | 0.000371 | 0.00251 |
| Alcoholism | hsa05034 | 20 | 179 | 0.000452 | 0.002974 |
| Hippo signaling pathway | hsa04390 | 18 | 154 | 0.000527 | 0.003419 |
| HTLV-I infection | hsa05166 | 25 | 259 | 0.000709 | 0.004375 |
| Notch signaling pathway | hsa04330 | 9 | 48 | 0.000736 | 0.004529 |
| Hepatitis C | hsa05160 | 16 | 133 | 0.000794 | 0.004799 |
| Focal adhesion | hsa04510 | 21 | 203 | 0.000824 | 0.004956 |
| Inositol phosphate metabolism | hsa00562 | 11 | 71 | 0.000827 | 0.004962 |
| Prolactin signaling pathway | hsa04917 | 11 | 72 | 0.000916 | 0.005352 |
| Arginine and proline metabolism | hsa00330 | 9 | 50 | 0.000951 | 0.005513 |
| Estrogen signaling pathway | hsa04915 | 13 | 99 | 0.001167 | 0.006583 |
| Melanogenesis | hsa04916 | 13 | 100 | 0.001267 | 0.00707 |
| cAMP signaling pathway | hsa04024 | 20 | 199 | 0.001488 | 0.008019 |
| Protein digestion and absorption | hsa04974 | 12 | 90 | 0.001581 | 0.008429 |
| Basal cell carcinoma | hsa05217 | 9 | 55 | 0.001718 | 0.008992 |
| EGFR tyrosine kinase inhibitor resistance | hsa01521 | 11 | 81 | 0.002141 | 0.010727 |
| Selenocompound metabolism | hsa00450 | 5 | 17 | 0.002178 | 0.010861 |
| Melanoma | hsa05218 | 10 | 71 | 0.002642 | 0.012742 |
| TGF-beta signaling pathway | hsa04350 | 11 | 84 | 0.002765 | 0.013183 |
| Endocrine resistance | hsa01522 | 12 | 97 | 0.002782 | 0.01325 |
| Dorso-ventral axis formation | hsa04320 | 6 | 28 | 0.003142 | 0.014698 |
| Aldosterone-regulated sodium reabsorption | hsa04960 | 7 | 39 | 0.003489 | 0.015961 |
| Herpes simplex infection | hsa05168 | 18 | 186 | 0.003607 | 0.016437 |
| Chemokine signaling pathway | hsa04062 | 18 | 187 | 0.003798 | 0.017195 |
| Hematopoietic cell lineage | hsa04640 | 11 | 88 | 0.003817 | 0.017263 |
| Tryptophan metabolism | hsa00380 | 7 | 40 | 0.003948 | 0.017598 |
| Prostate cancer | hsa05215 | 11 | 89 | 0.004124 | 0.018265 |
| Lysine degradation | hsa00310 | 8 | 52 | 0.004273 | 0.018772 |
| HIF-1 signaling pathway | hsa04066 | 12 | 103 | 0.004322 | 0.018943 |
| Thyroid hormone signaling pathway | hsa04919 | 13 | 118 | 0.004692 | 0.02039 |
| Toxoplasmosis | hsa05145 | 13 | 119 | 0.005003 | 0.021516 |
| Legionellosis | hsa05134 | 8 | 55 | 0.005771 | 0.023912 |
| ECM-receptor interaction | hsa04512 | 10 | 82 | 0.006618 | 0.026847 |
| ABC transporters | hsa02010 | 7 | 45 | 0.006965 | 0.027929 |
| Cysteine and methionine metabolism | hsa00270 | 7 | 45 | 0.006965 | 0.027929 |
| Acute myeloid leukemia | hsa05221 | 8 | 57 | 0.006972 | 0.027929 |
| Peroxisome | hsa04146 | 10 | 83 | 0.007135 | 0.028504 |
| Adipocytokine signaling pathway | hsa04920 | 9 | 70 | 0.00721 | 0.028693 |

| | | | | | |
|---|---|---|---|---|---|
| Cytokine-cytokine receptor interaction | hsa04060 | 22 | 265 | 0.007523 | 0.029798 |
| Inflammatory mediator regulation of TRP channels | hsa04750 | 11 | 98 | 0.007864 | 0.030617 |
| Alanine aspartate and glutamate metabolism | hsa00250 | 6 | 35 | 0.008121 | 0.031442 |
| Glycosphingolipid biosynthesis - lacto and neolacto series | hsa00601 | 5 | 26 | 0.010174 | 0.037761 |
| Natural killer cell mediated cytotoxicity | hsa04650 | 13 | 135 | 0.012616 | 0.044682 |
| Sphingolipid signaling pathway | hsa04071 | 12 | 121 | 0.01328 | 0.046632 |
| MicroRNAs in cancer | hsa05206 | 23 | 299 | 0.014109 | 0.048345 |
| Insulin signaling pathway | hsa04910 | 13 | 139 | 0.015478 | 0.052197 |
| Aldosterone synthesis and secretion | hsa04925 | 9 | 81 | 0.016259 | 0.054134 |
| AMPK signaling pathway | hsa04152 | 12 | 125 | 0.016465 | 0.054683 |
| RNA transport | hsa03013 | 15 | 172 | 0.016831 | 0.055118 |
| Wnt signaling pathway | hsa04310 | 13 | 143 | 0.018809 | 0.060254 |
| Glutamatergic synapse | hsa04724 | 11 | 114 | 0.020436 | 0.06469 |
| Huntington's disease | hsa05016 | 16 | 193 | 0.020656 | 0.06469 |
| Insulin secretion | hsa04911 | 9 | 85 | 0.021036 | 0.065383 |
| Amoebiasis | hsa05146 | 10 | 100 | 0.021533 | 0.066595 |
| AGE-RAGE signaling pathway in diabetic complications | hsa04933 | 10 | 101 | 0.022777 | 0.069597 |
| Calcium signaling pathway | hsa04020 | 15 | 180 | 0.023569 | 0.071684 |
| Glucagon signaling pathway | hsa04922 | 10 | 102 | 0.024071 | 0.073043 |
| cGMP-PKG signaling pathway | hsa04022 | 14 | 167 | 0.026908 | 0.079495 |
| Cocaine addiction | hsa05030 | 6 | 49 | 0.031476 | 0.089796 |
| Synaptic vesicle cycle | hsa04721 | 7 | 63 | 0.032031 | 0.090826 |
| Viral carcinogenesis | hsa05203 | 16 | 205 | 0.032441 | 0.091904 |
| Proteoglycans in cancer | hsa05205 | 16 | 205 | 0.032441 | 0.091904 |
| Ovarian steroidogenesis | hsa04913 | 6 | 50 | 0.034005 | 0.094755 |
| Caffeine metabolism | hsa00232 | 2 | 5 | 0.034217 | 0.094755 |
| Glioma | hsa05214 | 7 | 65 | 0.036576 | 0.098824 |
| Aminoacyl-tRNA biosynthesis | hsa00970 | 7 | 66 | 0.038999 | 0.104571 |
| Phospholipase D signaling pathway | hsa04072 | 12 | 144 | 0.039855 | 0.105692 |
| Glycosaminoglycan biosynthesis - keratan sulfate | hsa00533 | 3 | 15 | 0.040964 | 0.107372 |
| Amphetamine addiction | hsa05031 | 7 | 67 | 0.041525 | 0.108429 |
| Hepatitis B | hsa05161 | 12 | 146 | 0.043236 | 0.111925 |
| Vitamin B6 metabolism | hsa00750 | 2 | 6 | 0.044328 | 0.111925 |
| Osteoclast differentiation | hsa04380 | 11 | 132 | 0.047675 | 0.118419 |
| Protein processing in endoplasmic reticulum | hsa04141 | 13 | 166 | 0.049148 | 0.121063 |
| Regulation of lipolysis in adipocytes | hsa04923 | 6 | 56 | 0.051909 | 0.127111 |
| Non-small cell lung cancer | hsa05223 | 6 | 56 | 0.051909 | 0.127111 |
| Leukocyte transendothelial migration | hsa04670 | 10 | 118 | 0.052511 | 0.128347 |
| Epstein-Barr virus infection | hsa05169 | 15 | 204 | 0.055782 | 0.130732 |
| Systemic lupus erythematosus | hsa05322 | 11 | 136 | 0.056053 | 0.131301 |
| Neurotrophin signaling pathway | hsa04722 | 10 | 120 | 0.057179 | 0.133359 |
| B cell receptor signaling pathway | hsa04662 | 7 | 73 | 0.058893 | 0.136606 |
| Other glycan degradation | hsa00511 | 3 | 18 | 0.060693 | 0.138769 |
| Platelet activation | hsa04611 | 10 | 122 | 0.06211 | 0.141916 |
| Tight junction | hsa04530 | 11 | 139 | 0.062942 | 0.143409 |
| Other types of O-glycan biosynthesis | hsa00514 | 4 | 31 | 0.063846 | 0.144608 |
| Biosynthesis of amino acids | hsa01230 | 7 | 75 | 0.065542 | 0.147537 |
| Propanoate metabolism | hsa00640 | 4 | 32 | 0.069465 | 0.151175 |
| Carbohydrate digestion and absorption | hsa04973 | 5 | 46 | 0.069619 | 0.151258 |
| RNA degradation | hsa03018 | 7 | 77 | 0.072625 | 0.157046 |
| Hedgehog signaling pathway | hsa04340 | 5 | 47 | 0.074404 | 0.160515 |
| Apoptosis - multiple species | hsa04215 | 4 | 33 | 0.075328 | 0.161634 |
| Steroid biosynthesis | hsa00100 | 3 | 20 | 0.07587 | 0.161663 |
| Cholinergic synapse | hsa04725 | 9 | 111 | 0.0779 | 0.165488 |
| Valine leucine and isoleucine degradation | hsa00280 | 5 | 48 | 0.079364 | 0.166169 |
| Circadian entrainment | hsa04713 | 8 | 95 | 0.079558 | 0.166169 |
| Tyrosine metabolism | hsa00350 | 4 | 35 | 0.087772 | 0.179561 |
| Phosphatidylinositol signaling system | hsa04070 | 8 | 98 | 0.09041 | 0.1845 |
| Pancreatic cancer | hsa05212 | 6 | 66 | 0.092471 | 0.185911 |
| Glycolysis / Gluconeogenesis | hsa00010 | 6 | 67 | 0.09726 | 0.193277 |
| Mineral absorption | hsa04978 | 5 | 52 | 0.100902 | 0.19956 |
| Endometrial cancer | hsa05213 | 5 | 52 | 0.100902 | 0.19956 |
| Choline metabolism in cancer | hsa05231 | 8 | 101 | 0.102072 | 0.200801 |
| Fc epsilon RI signaling pathway | hsa04664 | 6 | 68 | 0.102178 | 0.200801 |
| Ubiquitin mediated proteolysis | hsa04120 | 10 | 137 | 0.107692 | 0.207883 |
| Small cell lung cancer | hsa05222 | 7 | 86 | 0.109841 | 0.211319 |
| Histidine metabolism | hsa00340 | 3 | 24 | 0.110548 | 0.211614 |
| RIG-I-like receptor signaling pathway | hsa04622 | 6 | 70 | 0.112395 | 0.214746 |
| Chagas disease (American trypanosomiasis) | hsa05142 | 8 | 104 | 0.114531 | 0.218011 |

| | | | | | |
|---|---|---|---|---|---|
| Thyroid hormone synthesis | hsa04918 | 6 | 71 | 0.11769 | 0.223052 |
| T cell receptor signaling pathway | hsa04660 | 8 | 105 | 0.118859 | 0.22508 |
| Gap junction | hsa04540 | 7 | 88 | 0.119267 | 0.225715 |
| Fatty acid elongation | hsa00062 | 3 | 25 | 0.120021 | 0.225893 |
| Pyruvate metabolism | hsa00620 | 4 | 40 | 0.122807 | 0.227762 |
| Cell cycle | hsa04110 | 9 | 124 | 0.1254 | 0.232008 |
| Chronic myeloid leukemia | hsa05220 | 6 | 73 | 0.128646 | 0.237773 |
| Tuberculosis | hsa05152 | 12 | 179 | 0.128995 | 0.238371 |
| NOD-like receptor signaling pathway | hsa04621 | 5 | 57 | 0.131451 | 0.240774 |
| Fatty acid biosynthesis | hsa00061 | 2 | 13 | 0.136329 | 0.246461 |
| Ascorbate and aldarate metabolism | hsa00053 | 3 | 27 | 0.139806 | 0.25082 |
| Phototransduction | hsa04744 | 3 | 27 | 0.139806 | 0.25082 |
| Platinum drug resistance | hsa01524 | 6 | 75 | 0.140073 | 0.251052 |
| Fc gamma R-mediated phagocytosis | hsa04666 | 7 | 93 | 0.144571 | 0.258913 |
| Glycerolipid metabolism | hsa00561 | 5 | 59 | 0.144711 | 0.259012 |
| Serotonergic synapse | hsa04726 | 8 | 112 | 0.151497 | 0.26625 |
| Glycosphingolipid biosynthesis - globo series | hsa00603 | 2 | 14 | 0.151522 | 0.26625 |
| Long-term depression | hsa04730 | 5 | 60 | 0.151548 | 0.26625 |
| Adrenergic signaling in cardiomyocytes | hsa04261 | 10 | 149 | 0.154941 | 0.271494 |
| Carbon metabolism | hsa01200 | 8 | 113 | 0.156481 | 0.273723 |
| Hippo signaling pathway -multiple species | hsa04392 | 3 | 29 | 0.160592 | 0.279422 |
| Pancreatic secretion | hsa04972 | 7 | 96 | 0.160882 | 0.279661 |
| Non-alcoholic fatty liver disease (NAFLD) | hsa04932 | 10 | 151 | 0.16369 | 0.28395 |
| Colorectal cancer | hsa05210 | 5 | 62 | 0.165616 | 0.286802 |
| Nicotinate and nicotinamide metabolism | hsa00760 | 3 | 30 | 0.171316 | 0.292913 |
| Progesterone-mediated oocyte maturation | hsa04914 | 7 | 98 | 0.172196 | 0.294253 |
| Endocrine and other factor-regulated calcium reabsorption | hsa04961 | 4 | 47 | 0.179927 | 0.306266 |
| Sphingolipid metabolism | hsa00600 | 4 | 47 | 0.179927 | 0.306266 |
| Mucin type O-Glycan biosynthesis | hsa00512 | 3 | 31 | 0.182236 | 0.306971 |
| Amino sugar and nucleotide sugar metabolism | hsa00520 | 4 | 48 | 0.18872 | 0.316073 |
| Type II diabetes mellitus | hsa04930 | 4 | 48 | 0.18872 | 0.316073 |
| Vascular smooth muscle contraction | hsa04270 | 8 | 120 | 0.193437 | 0.322794 |
| Long-term potentiation | hsa04720 | 5 | 66 | 0.19519 | 0.325542 |
| Primary bile acid biosynthesis | hsa00120 | 2 | 17 | 0.198744 | 0.32872 |
| Phenylalanine metabolism | hsa00360 | 2 | 17 | 0.198744 | 0.32872 |
| Central carbon metabolism in cancer | hsa05230 | 5 | 67 | 0.202856 | 0.334977 |
| Amyotrophic lateral sclerosis (ALS) | hsa05014 | 4 | 51 | 0.215869 | 0.349197 |
| SNARE interactions in vesicular transport | hsa04130 | 3 | 34 | 0.216001 | 0.349197 |
| Toll-like receptor signaling pathway | hsa04620 | 7 | 106 | 0.220603 | 0.354295 |
| ErbB signaling pathway | hsa04012 | 6 | 88 | 0.224333 | 0.354295 |
| GABAergic synapse | hsa04727 | 6 | 88 | 0.224333 | 0.354295 |
| African trypanosomiasis | hsa05143 | 3 | 35 | 0.227536 | 0.354295 |
| Salivary secretion | hsa04970 | 6 | 89 | 0.231416 | 0.354295 |
| Cell adhesion molecules (CAMs) | hsa04514 | 9 | 146 | 0.232694 | 0.354295 |
| Bile secretion | hsa04976 | 5 | 71 | 0.234456 | 0.354762 |
| Pentose and glucuronate interconversions | hsa00040 | 3 | 36 | 0.239183 | 0.360503 |
| PPAR signaling pathway | hsa03320 | 5 | 72 | 0.242564 | 0.36542 |
| Rheumatoid arthritis | hsa05323 | 6 | 91 | 0.245786 | 0.369788 |
| One carbon pool by folate | hsa00670 | 2 | 20 | 0.247388 | 0.370134 |
| Glycosaminoglycan biosynthesis - chondroitin sulfate / dermatan sulfate | hsa00532 | 2 | 20 | 0.247388 | 0.370134 |
| Pathogenic Escherichia coli infection | hsa05130 | 4 | 55 | 0.253542 | 0.377924 |
| Fanconi anemia pathway | hsa03460 | 4 | 55 | 0.253542 | 0.377924 |
| Adherens junction | hsa04520 | 5 | 74 | 0.258996 | 0.380865 |
| NF-kappa B signaling pathway | hsa04064 | 6 | 93 | 0.260405 | 0.380865 |
| Pertussis | hsa05133 | 5 | 75 | 0.267309 | 0.380927 |
| Regulation of autophagy | hsa04140 | 3 | 40 | 0.286589 | 0.404693 |
| Nicotine addiction | hsa05033 | 3 | 40 | 0.286589 | 0.404693 |
| Bacterial invasion of epithelial cells | hsa05100 | 5 | 78 | 0.292575 | 0.406051 |
| Antigen processing and presentation | hsa04612 | 5 | 78 | 0.292575 | 0.406051 |
| Biosynthesis of unsaturated fatty acids | hsa01040 | 2 | 23 | 0.296367 | 0.406051 |
| Bladder cancer | hsa05219 | 3 | 41 | 0.298573 | 0.406051 |
| Oxytocin signaling pathway | hsa04921 | 9 | 158 | 0.301824 | 0.4095 |
| VEGF signaling pathway | hsa04370 | 4 | 61 | 0.312149 | 0.420473 |
| Retrograde endocannabinoid signaling | hsa04723 | 6 | 101 | 0.320797 | 0.428438 |
| Arachidonic acid metabolism | hsa00590 | 4 | 62 | 0.32206 | 0.428438 |
| Fatty acid degradation | hsa00071 | 3 | 44 | 0.33463 | 0.434229 |
| Vasopressin-regulated water reabsorption | hsa04962 | 3 | 44 | 0.33463 | 0.434229 |
| Taste transduction | hsa04742 | 5 | 83 | 0.335474 | 0.435078 |
| Renin secretion | hsa04924 | 4 | 64 | 0.341941 | 0.443151 |
| Maturity onset diabetes of the young | hsa04950 | 2 | 26 | 0.34484 | 0.445649 |
| Ether lipid metabolism | hsa00565 | 3 | 45 | 0.346643 | 0.447475 |

| | | | | | |
|---|---|---|---|---|---|
| Salmonella infection | hsa05132 | 5 | 86 | 0.361476 | 0.4536 |
| Alzheimer's disease | hsa05010 | 9 | 168 | 0.362661 | 0.4549 |
| Butanoate metabolism | hsa00650 | 2 | 28 | 0.376553 | 0.470076 |
| Fatty acid metabolism | hsa01212 | 3 | 48 | 0.382511 | 0.472353 |
| Dopaminergic synapse | hsa04728 | 7 | 130 | 0.385328 | 0.472353 |
| Synthesis and degradation of ketone bodies | hsa00072 | 1 | 10 | 0.38641 | 0.472353 |
| GnRH signaling pathway | hsa04912 | 5 | 91 | 0.404857 | 0.492475 |
| Citrate cycle (TCA cycle) | hsa00020 | 2 | 30 | 0.40761 | 0.493684 |
| Taurine and hypotaurine metabolism | hsa00430 | 1 | 11 | 0.413063 | 0.493684 |
| Spliceosome | hsa03040 | 7 | 134 | 0.413895 | 0.494614 |
| Glutathione metabolism | hsa00480 | 3 | 52 | 0.42957 | 0.510288 |
| Glycerophospholipid metabolism | hsa00564 | 5 | 95 | 0.439305 | 0.512429 |
| Base excision repair | hsa03410 | 2 | 33 | 0.452716 | 0.526293 |
| Non-homologous end-joining | hsa03450 | 1 | 13 | 0.462947 | 0.530164 |
| Prion diseases | hsa05020 | 2 | 35 | 0.481671 | 0.547988 |
| Lysosome | hsa04142 | 6 | 123 | 0.490886 | 0.55257 |
| Oocyte meiosis | hsa04114 | 6 | 123 | 0.490886 | 0.55257 |
| Glycosphingolipid biosynthesis - ganglio series | hsa00604 | 1 | 15 | 0.508594 | 0.565358 |
| Viral myocarditis | hsa05416 | 3 | 60 | 0.519209 | 0.575623 |
| Hypertrophic cardiomyopathy (HCM) | hsa05410 | 4 | 83 | 0.525731 | 0.581799 |
| Purine metabolism | hsa00230 | 8 | 176 | 0.549076 | 0.599938 |
| Fat digestion and absorption | hsa04975 | 2 | 41 | 0.562575 | 0.612159 |
| 2-Oxocarboxylic acid metabolism | hsa01210 | 1 | 18 | 0.569897 | 0.615889 |
| Shigellosis | hsa05131 | 3 | 65 | 0.571183 | 0.616842 |
| Porphyrin and chlorophyll metabolism | hsa00860 | 2 | 42 | 0.575147 | 0.620539 |
| Dilated cardiomyopathy | hsa05414 | 4 | 90 | 0.587225 | 0.631028 |
| Glycosaminoglycan degradation | hsa00531 | 1 | 19 | 0.588584 | 0.631028 |
| Epithelial cell signaling in Helicobacter pylori infection | hsa05120 | 3 | 68 | 0.600639 | 0.642751 |
| mRNA surveillance pathway | hsa03015 | 4 | 92 | 0.603916 | 0.646031 |
| Drug metabolism - other enzymes | hsa00983 | 2 | 46 | 0.622767 | 0.661718 |
| Arginine biosynthesis | hsa00220 | 1 | 21 | 0.623557 | 0.661718 |
| Metabolism of xenobiotics by cytochrome P450 | hsa00980 | 3 | 73 | 0.646683 | 0.68192 |
| Proximal tubule bicarbonate reclamation | hsa04964 | 1 | 23 | 0.655559 | 0.687708 |
| Mismatch repair | hsa03430 | 1 | 23 | 0.655559 | 0.687708 |
| N-Glycan biosynthesis | hsa00510 | 2 | 49 | 0.655695 | 0.687708 |
| Vitamin digestion and absorption | hsa04977 | 1 | 24 | 0.670525 | 0.70006 |
| alpha-Linolenic acid metabolism | hsa00592 | 1 | 25 | 0.684841 | 0.712655 |
| Complement and coagulation cascades | hsa04610 | 3 | 79 | 0.696786 | 0.724031 |
| Phagosome | hsa04145 | 6 | 155 | 0.704373 | 0.729833 |
| Chemical carcinogenesis | hsa05204 | 3 | 82 | 0.719735 | 0.742898 |
| Glyoxylate and dicarboxylate metabolism | hsa00630 | 1 | 28 | 0.724167 | 0.746632 |
| Staphylococcus aureus infection | hsa05150 | 2 | 57 | 0.732262 | 0.754554 |
| Linoleic acid metabolism | hsa00591 | 1 | 29 | 0.736154 | 0.757543 |
| Steroid hormone biosynthesis | hsa00140 | 2 | 58 | 0.740738 | 0.76209 |
| Galactose metabolism | hsa00052 | 1 | 31 | 0.758588 | 0.777663 |
| Ribosome biogenesis in eukaryotes | hsa03008 | 3 | 89 | 0.767993 | 0.786689 |
| RNA polymerase | hsa03020 | 1 | 32 | 0.769079 | 0.786923 |
| Fructose and mannose metabolism | hsa00051 | 1 | 33 | 0.779115 | 0.79586 |
| Morphine addiction | hsa05032 | 3 | 91 | 0.780469 | 0.797106 |
| Cytosolic DNA-sensing pathway | hsa04623 | 2 | 64 | 0.786896 | 0.803182 |
| Retinol metabolism | hsa00830 | 2 | 65 | 0.793845 | 0.809284 |
| Inflammatory bowel disease (IBD) | hsa05321 | 2 | 66 | 0.800592 | 0.814985 |
| Primary immunodeficiency | hsa05340 | 1 | 37 | 0.815085 | 0.827534 |
| Drug metabolism - cytochrome P450 | hsa00982 | 2 | 69 | 0.81967 | 0.832006 |
| Leishmaniasis | hsa05140 | 2 | 74 | 0.847849 | 0.857477 |
| Gastric acid secretion | hsa04971 | 2 | 74 | 0.847849 | 0.857477 |
| Arrhythmogenic right ventricular cardiomyopathy (ARVC) | hsa05412 | 2 | 74 | 0.847849 | 0.857477 |
| Pyrimidine metabolism | hsa00240 | 3 | 105 | 0.853017 | 0.862133 |
| Basal transcription factors | hsa03022 | 1 | 45 | 0.870412 | 0.878553 |
| Parkinson's disease | hsa05012 | 4 | 142 | 0.882593 | 0.889869 |
| Malaria | hsa05144 | 1 | 49 | 0.89152 | 0.898179 |
| Intestinal immune network for IgA production | hsa04672 | 1 | 50 | 0.896237 | 0.902732 |
| Autoimmune thyroid disease | hsa05320 | 1 | 54 | 0.91314 | 0.918749 |
| Starch and sucrose metabolism | hsa00500 | 1 | 57 | 0.923986 | 0.929152 |
| Ribosome | hsa03010 | 3 | 138 | 0.947254 | 0.950674 |
| Olfactory transduction | hsa04740 | 2 | 420 | 1 | 1 |